Natural antioxidants and their use in Food Technology

Shweta Gautam, Ph.D.

Doctoral Thesis Summary

Tomas Bata University in Zlín

Univerzita Tomáše Bati ve Zlíně
Fakulta technologická

Department of Food Technology

Doctoral Thesis Summary

Natural antioxidants and their use in Food Technology

Přírodní antioxidanty a jejich využití v Potravinářství

Author:	**Shweta Gautam, Ph.D.**
Degree programme:	P0721D210006 Chemistry, Technology and Analysis of Food
Supervisor:	Prof. Ing. Lubomír Lapčík, CSc.
Consultant:	Doc. Mgr. Barbora Lapčíková, Ph.D.
External Examiners:	doc. Ing. Eva Vítová, Ph.D. prof. Ing. Marián Valko, DrSc.

Zlín, August

Published by **Tomas Bata University in Zlín** in the Edition **Doctoral Thesis Summary.**
The publication was issued in the year 2025

Klíčová slova: *přírodní antioxidanty, esenciální oleje, karboxymethyl celulóza, síťování, zapouzdření*

Key words: *natural antioxidants, essential oils, carboxymethyl cellulose, cross-linking, encapsulation*

Full text of the doctoral thesis is available in the Library of TBU in Zlín.

ISBN: 978-80-7678-350-8

ABSTRAKT

Cílem této studie bylo vyvinout zesítěný, biologicky rozložitelný aktivní obalový materiál na bázi polysacharidů obsahující zapouzdřené éterické oleje (EO). Výzkum byl proveden v několika fázích, aby bylo možné tohoto cíle dosáhnout. Nejprve byl na základě matematického modelování vytvořen systematický experimentální návrh pro formulaci složení fólie, ve které byly koncentrace jednotlivých složek optimálně vyváženy. Následně byly připraveny fólie s použitím EO jak jednotlivě, tak v kombinaci, a byly podrobeny komplexním fyzikálním, chemickým, mechanickým, optickým a mikrobiologickým analýzám. Výsledky ukázaly, že fólie vykazovaly vysokou antioxidační aktivitu při teplotách 4 °C i 25 °C, nízkou propustnost vodní páry a vysoký stupeň zesíťování (~99 %), což svědčí o vynikající odolnosti proti vlhkosti. Byla zaznamenána antibakteriální aktivita proti gramnegativním bakteriím a díky kontrolovaným poměrům polymeru a síťovacího činidla bylo dosaženo mírných tahových a elastických vlastností.

V závěrečné fázi byly vybrané složení fólií aplikovány na vzorky mletého kuřecího a hovězího masa. Fólie prokázaly lepší inhibici mikroorganismů v hovězím mase, zpomalily primární oxidaci v obou druzích masa a účinně kontrolovaly sekundární oxidaci, zejména ve vzorcích obsahujících oleje z oregana a tymiánu. Multivariační a korelační analýzy dále potvrdily, že antioxidační kapacita fólie byla silně spojena s inhibicí mikrobiálního růstu, zejména u hovězího masa. Tyto výsledky potvrdily potenciál fólií jako ekologické alternativy k běžným plastovým obalům se slibnými možnostmi použití při konzervaci rychle se kazících potravin. Studie poskytuje základ pro budoucí optimalizaci a škálovatelnost aktivních obalů na bázi biopolymerů v potravinářském průmyslu.

ABSTRACT

The aim of this study was to develop a crosslinked, polysaccharide-based biodegradable active packaging material incorporating encapsulated essential oils (EOs). The research was conducted in multiple phases to achieve this objective. Initially, a systematic experimental design was established based on mathematical modelling to formulate film compositions in which the concentrations of individual components were optimally balanced. Subsequently, films were prepared using EOs both individually and in combination, and were subjected to comprehensive physical, chemical, mechanical, optical, and microbiological analyses. The results revealed that the films exhibited high antioxidant activity at both 4 °C and 25 °C, low water vapour permeability, and a high degree of crosslinking (~99%), indicating excellent resistance to moisture. Antibacterial activity was noted against gram-negative bacteria, and moderate tensile and elastic properties were achieved through controlled polymer–crosslinker ratios.

In the final phase, selected film formulations were applied to ground chicken and beef samples. The films demonstrated better microbial inhibition in beef, delayed primary oxidation in both meats, and effective control of secondary oxidation, particularly in samples containing oregano and thyme oils. Multivariate and correlation analyses further confirmed that film antioxidant capacity was strongly associated with microbial inhibition, especially in beef. These findings supported the films' potential as eco-friendly alternatives to conventional plastic packaging, with promising applications in preserving perishable food products. The study provides a foundation for future optimization and scalability of biopolymer-based active packaging in the food industry.

CONTENTS

1 CURRENT STATE OF THE ISSUE

1.1 Essential Oils

Essential oils (EOs) are naturally occurring complex compounds capable of antioxidant properties but not directly placed under any specific category in NAs. EOs are mixtures of volatile compounds containing terpenes, terpenoids, phenolics and other aromatic compounds. EOs have remarkable antioxidant properties and are considered secondary metabolites of the plants, produced to protect them against pest infestations and environmental stresses (Sharma et al. 2021).

1.2 Regulatory Aspect

The European Commission has registered EO bioactive components as commercial flavouring agents. Some commonly used natural flavouring agents include cinnamaldehyde, citral, thymol, menthol, carvone, limonene, eugenol, and carvacrol, which have no adverse effects on human health. The European Union (EU) ensures the safety of these natural agents through rigorous toxicological and microbial tests before registration (EUROPEAN COMMISSION (EU) 2021). Once approved, these registered flavours are added to the Everything Added to Food in the United States (EAFUS) list. This list, sanctioned by the Food and Drug Administration, also includes food additives with Generally Recognised as Safe (GRAS) status. However, there are exceptions, such as estragole, which, despite being on the EAFUS list, is prohibited by the EU due to its genotoxic and carcinogenic properties.

1.3 Current applications of EOs in food technology

The natural antibacterial and antioxidant action of EOs has prompted an increase in research to use the EOs as replacements for chemical preservatives like BHT and BHQs in fresh and processed foods. However, the presence of

fats in food reduces the bioactive potential of EOs in seafood, similar to meat and meat products. According to Speranza, Corbo (2010), 0.05% volume by weight of oregano EO showed a synergistic effect with the fat in cod fillets against *Photobacterium phosphoreum* in cod fillets than in salmon, due to the higher fatty profile of salmon (Speranza, Corbo 2010). Numerous studies have proved that the synergetic effect of EO combinations improves microbial stability of fat-rich seafood products (Hassoun, Çoban 2017).

Additionally, EOs are also being studied to develop ECs and active packaging materials or EFs, simultaneously attempting to reduce the use of plastics. Modern innovations have revolutionised EFs and ECs (Gautam, Lapčík et al. 2023, Dos Santos et al. 2023, Mei et al. 2021, Sun, J. et al. 2023). These biopolymeric packaging materials are designed to emulate the properties and functionalities of traditional packaging materials like plastic films and coatings (Murtaja et al. 2022, Hu 2014, Huang et al. 2020, Sun, R. et al. 2021). Additionally, the films can be used as carriers for functional ingredients, such as EOs, further enhancing food preservation.

According to the literature analysis, EFs and ECs can be used for fresh and processed foods such as fruits and vegetables, fresh and processed meat and seafood, and solid dairy products such as cheese. In addition to the antimicrobial properties, the EOs also act as a plasticising agent and enhance water vapour permeability, mechanical properties, UV properties and gas permeability properties of the EFs.

2 Aim of thesis

The main aim of this study is to develop an effective biodegradable active packaging material with encapsulated EOs, both individually and in combinations. The study will evaluate the physical, chemical, mechanical, optical, and microbiological properties of the packaging material to determine its suitability for specific food groups. Additionally, the efficiency of this packaging on food products will be tested. To achieve this goal, the following sub-goals will be fulfilled:

- **Experimental design:** Create and implement an experimental design with varying concentrations of the ingredients to identify optimal combinations.
- **Analyse ingredients and interactions:** The individual components of the film and their interactions will be analysed, focusing on key characteristics such as crosslinking efficiency, antibacterial properties, and mechanical strength.
- **Preliminary film assessment and film optimisation:** Assess the preliminary films to refine the formulation and optimise the properties.
- **Analyse the and apply them to the food model:** Develop the films based on the formula and analyse their characteristics. Test the efficiency of the films on a food product.

3 Description of individual experiments

The methodology section of this thesis is divided into four sub-experiments described in this chapter.

3.1 Experiment I

The main aim of this experiment was to create a functional DOE using the Central Composite Design (CCD) in the Design Expert software. The variables and the concentration range of the ingredients were decided based on a literature review and preliminary trial runs. The base material was developed from Sodium carboxymethyl cellulose (CMCNa) and hydroxyethyl cellulose (HEC) in the ratio of 3:1, as per the works of Demitri et al. (2008), crosslinked with citric acid (CA) and encapsulation with three EOs, namely Thyme, Clove and Oregano. CCD was used with the following variable concentration ranges: total polymer concentration (4.5-7.5 g) and CA (15-20 % of the wt. of the polymer). Based on the previous experiments (Gautam, Lapcik et al. 2023) the concentration of EOs was 3% (w/v) and glycerol at 25% (w/v) of the total weight of the polymer. Tween 80 (T80) was used as a surfactant in the same concentration as that of EOs.

3.2 Experiment II

This experiment aimed to develop the emulsions and films based on the DOE. The determined concentration of the polymers (CMCNa and HEC) was dissolved in 100 mL distilled water (DW) and allowed to hydrate till the solution was clear. Other ingredients were added to the polymer solution and homogenised using a homogeniser at 20000 RPM for 20 minutes. The emulsions were centrifuged at 6000 RPM for 20 mins to remove all the bubbles. The prepared emulsions were used to cast a uniform layer of films using Elcometer 3581 casting knife (Elcometer Limited, Manchester, UK) on a flat glass surface. The film layer was allowed to dry at 45 ℃ for 2 h and

crosslinked at 80 ℃ for 8 h. The dried films were cooled down and equilibrated at lab temperatures and humidity for easy peeling. The peeled films were stored between baking paper in standard lab conditions.

The prepared preliminary films were tested for their mechanical properties (tensile strength (TS), Young's modulus of elasticity (EM) and elongation at break (EB)) according to the ASTM standard method D882 (ASTM: D-882-91 method 1996) and swelling ratio. The obtained values of all the films were implemented into the software to check for inconsistencies before analysis.

3.3 Experiment III

The aim of this experiment was to analyse the obtained results to fit a regression model, assess the model adequacy, analyse the effect of factors and their interactions, and finally, run the optimisation tool to find the optimal factor levels.

3.4 Experiment IV

The main aim of this experiment was the validation of the results experimentally. The theoretically obtained formula was tested to confirm the model's accuracy.

The confirmatory runs were measured and compared with predicted values to validate the formula. Once the formula was validated, it was used to make the emulsions (100 mL) for a total of seven films as follows and tested for their physico-chemical and microbiological properties:

Table 1: Final composition of the bioactive films.

Sample names and codes	Total polymer	Citric acid 16.41%	Oil 3% (w/v) (ml)	Tween 80 3%	Glycerol 25%

	(CMCNa + HEC) (g)	(w/w) (g)		(w/v) (ml)	(w/v) (ml)
Control (CON)	6.82	1.12	-	-	1.353
Thyme (T)	6.82	1.12	0.147	0.193	1.353
Clove (C)	6.82	1.12	0.147	0.193	1.353
Oregano (O)	6.82	1.12	0.147	0.193	1.353
Thyme-Clove (TC)	6.82	1.12	0.073 + 0.073	0.193	1.353
Thyme-Oregano (TO)	6.82	1.12	0.073 + 0.073	0.193	1.353
Oregano-Clove (OC)	6.82	1.12	0.073 + 0.073	0.193	1.353

3.5 Selected processing methods

3.5.1 Scanning Electron Microscopy (SEM) and Confocal Laser Microscopy (CLSM)

SEM of the prepared films was performed on the Phenom XL G2 Scanning Electron Microscope (Thermo Fisher Scientific, Waltham, MA, USA). SEM Images were coated with gold and palladium in a SC7620 Mini metal sputter (Quorum Technologies, Lewes, UK) for 60 seconds. Electron microscope images were taken at an accelerating voltage of 5 kV, in secondary electron imaging mode and low beam intensity.

The visualisation of oil reservoirs in the film was performed using a confocal laser scanning microscope Olympus FLUOVIEW FV3000 (Olympus Corporation, Tokyo, Japan) equipped with a UPLSAPO 60x objective. Imaging was performed at 1× and 3× digital zoom using the proprietary FV31S-SW software (Olympus Corporation, Tokyo, Japan).

3.5.2 Light transmittance and opacity

The light transmittance of the film samples was measured using an ultraviolet spectrophotometer (Cecil CE 1021, Cambridge, United Kingdom) according to the method described by Cai et al. (2020). Films were cut into 4.5 cm × 1 cm and placed directly in the test cell. An empty cell was used as the reference. The measurement was carried out at the wavelengths of 280, 350, 400, 500, 600, 700 and 800 nm. Opacity was calculated using the following formula:

$$T = \frac{Abs_{600}}{d} \quad (1)$$

where Abs_{600} is the absorbance value at 600 nm and d is the thickness of the films (mm).

3.5.3 Antioxidant activity

The release of active compounds from the prepared films was carried out at temperatures of 4 °C and 25 °C. The food simulants were selected according to the European regulations: 3% v/v acetic acid (AA-Food simulant B) as an acidic food simulant (pH 4.5); 10% v/v ethanol (10% EtOH-Food simulant A) as an aqueous food simulant; and 50% v/v ethanol (50% EtOH-Food stimulant D1) as a simulant for foods with a lipophilic character. Distilled water (DW) was also selected as a control food simulant for comparison. A 4 × 4 cm film specimen was immersed in 10 mL simulant solution at the predetermined temperatures. The liquid was collected at 2, 4,

6, 8, 10, 12, 24 and 48 hours. The antioxidant activity was measured with a standard antioxidant assay using DPPH at 517 nm wavelength. The percentage inhibition values were calculated according to the following equation:

$$\%\ Inhibition = \frac{A_{blank} - A_{sample}}{A_{blank}} \times 100 \quad (2)$$

where A_{blank} is the absorbance of the methanolic solution of DPPH, and A_{sample} is the absorbance of the samples.

3.5.4 Mechanical testing

Tensile strength (TS), elongation at break (EB) and Young's modulus of elasticity (EM) were measured on Shimadzu AGS-100kNX (Shimadzu Corporation, Kyoto, Japan) according to the ASTM standard method D882 (ASTM International 2009). The applied strain rate was 5 mm/min, and the sample size with the dimensions 20 × 30 × 0.1 mm (length × width × thickness) was used.

3.5.5 Water Vapor Permeability-Water vapor Transmission Rate

WVP of the films was measured according to the standard method ASTM E96-95 (ASTM International 2013). Films were fixed on top of Payne permeability cups (Elcometer, Manchester, UK) containing (10 ± 1) g anhydrous calcium chloride. The cups were weighed and then placed in a desiccator filled with distilled water at 25 °C and a relative humidity of 75%. The weight of the test cups was measured after 48 h. The water vapour permeability (WVP) ($gm^{-1}s^{-1}Pa^{-1}$) and water vapour transmission rate (WVTR) ($gm^{-2}h$) were calculated using the following equations:

$$WVP = \frac{\Delta W \times d}{A \times \Delta P} \quad (3)$$

$$WVTR = \frac{\Delta W}{A \times t} \quad (4)$$

where ΔW is the weight change before and after the test (g); A is the test area (m^2); d is the thickness of films (mm); ΔP is the partial pressure difference across the films (kPa); t is the test time (h).

3.5.6 Moisture Absorption Kinetics

The moisture absorption kinetics was carried out as per the protocol established by Shen, Kamdem (2015). The films were cut into square pieces (2 × 2 cm) and conditioned using anhydrous calcium chloride at 0% relative humidity (RH) for 48 h. The films were weighed accurately (W_1) and conditioned at (23 ± 2) °C and 97% RH. The weight of samples was recorded every week (W_2) for 4 weeks to obtain the percentage of moisture absorption. The following formula was used to calculate the moisture uptake value:

$$\%\ Moisture\ uptake = \frac{W_2 - W_1}{W_1} \times 100 \quad (5)$$

The resulting values were fit with a first-order kinetics reaction to calculate the moisture absorption rate, absorption equilibrium ($c0$) and rate constant (k).

3.5.7 Swelling ratio

The swelling studies were conducted as per the works of Juncu et al. (2016) with slight modifications. Accurately weighed 2 × 2 cm films were immersed in 20 mL phosphate buffer solution of pH 7.4 at room temperature (23.5 ± 0.5) °C for 24 h. The films were carefully removed from the solution, and excess solution was wiped off with filter paper before weighing. The swelling ratio (SR) was calculated using the following formula:

$$SR = \frac{W_t - W_d}{W_d} \quad (6)$$

where W_t is the weight of the swollen film and W_d is the weight of the dried film.

3.5.8 Gel Fraction

Gel fraction was carried out by drying 2 × 2 cm films till they reached a constant weight (W_1) followed by boiling in double-distilled water for 5 min. The insoluble part of the films was washed again in distilled water and dried to a constant weight (W_2). The percentage gel fraction was calculated using the following formula ((Nordin et al. 2018):

$$\%\ Gel\ fraction = \frac{W_2}{W_1} \times 100 \quad (7)$$

3.5.9 Thermogravimetric analysis

Thermogravimetric analysis (TGA) was carried out on Discovery SDT 650B-TA Instruments (New Castle, DE, USA) according to the ASTM standard method D3418 (ASTM International 2003). The samples were cut into tiny circles to fit the aluminium pans. Three film layers were placed (weight = (10.0 ± 1.2) mg) in an open pan. The conditions of the experiment were set as follows: heat flow 10 °C/min and dynamic atmosphere of nitrogen (N2 = 100 mL/min); the temperature range was from 30 °C to 600 °C. The data obtained were then analysed using the Thermal Analysis Universal 2000 version 4.5A software (TA Instrument, New Castle, DE, USA).

3.5.10 Fourier Transform Infrared Spectroscopy

Infrared analysis was performed on Bruker IFS 55 FT-IR (Billerica, MA, USA) spectrometer equipped with attenuated total reflection accessory-Golden Gate-with diamond as the ATR element, single-reflection, and an incident angle of 45°. Measurements were recorded in the wavenumber range of 4000 to 500 cm^{-1}, with an interval of 4 cm^{-1}. The observed spectra were

ATR corrected by Kubelka-Munk conversions. Chemometric analyses of the ATR-FT-IR spectra were performed using Opus software (Bruker, Billerica, MA, USA). The graphs were normalised using OriginPro 9.0 (OriginLab, Northampton, MA, USA).

3.5.11 Biodegradability in soil

The biodegradability of films was conducted as per the works of (Rachmawati et al. 2015) with slight modifications. The film samples (2 × 2 cm) were weighed (W_1) and buried at 6 cm depth in plastic cups (d = 6.2 cm) containing substrate purchased from the local market. The cups were sprinkled with distilled water to maintain 50-60% moisture and stored at (23.5 ± 0.5) °C for 6 weeks. Films were visually observed and weighed (W_2) every week. The percentage of degradation was calculated using the following formula:

$$\%\, Weight\ loss = \frac{W_1 - W_2}{W_1} \times 100 \quad (8)$$

3.5.12 Antimicrobial activity analysis

The antimicrobial activity of the films was determined using the agar disk diffusion method. *E. coli* and *S. aureus* were selected as the Gram-positive and Gram-negative candidate bacteria, respectively. From the pure bacterial cultures, some colonies were picked and inoculated in 15 mL of nutrient broth at 37 °C for 24 h. The next day, the inoculated broth was serially diluted to 10-4 for each bacterium. 100 µL of each dilution was then used to inoculate nutrient agar plates. Sterile circular films (10 mm diameter) were carefully placed on the surface of the inoculated plates and incubated at 37 °C for 24 h. The diameter of the bacteriostatic zone was measured using a micrometre calliper.

3.5.13 Shelf-Life study

The efficiency of the prepared films as a suitable packaging material for extending the shelf-life of food products was evaluated on minced beef and minced chicken meat. Fresh ground meat was purchased from the local market with a "use-by" date expiring in 4 days. About (10 ± 1) g of meat sample was rolled in a 3 × 9 cm film, placed in a plastic cup and sealed with Polyvinyl Chloride wrap to mimic the commercial packaging of minced meat. One sample was packed in parchment paper (to mimic commercial packaging) and considered as control 1, whereas the sample packed with control film was considered as control 2. The entire procedure was conducted in a sterile environment. The films were treated under a UV lamp for 45 min on each side prior to use. The packaged samples were stored at (4.2 ± 0.8) °C for 6 days and studied for microbial spoilage, peroxide value analysis, Thio barbituric acid analysis and colour change on 0, 2, 4 and 6 days.

3.5.13.1 Microbial study

Minced chicken and beef samples (10 g) were placed in 90 mL of sterile physiological solution and homogenised using a BagMixer 400 stomacher (Interscience, Chemin du Bois des Arpents, Saint-Nom-la-Bretèche, France) at a speed of 8 strokes/sec for 3 min. For microbiological enumeration, serial dilutions (1:10) were prepared in sterile physiological solution. 100 µL of it was plated on Plate Count Agar (PCA) to enumerate psychrotrophic bacteria at 7 °C for 5 days.

3.5.13.2 Thio barbituric acid analysis (TBARS)

TBARS was evaluated based on the works of Kim et al. (2022) with slight modifications. 5 g of mined meat sample was mixed with 15 mL Perchloric acid (3.86%) and 0.5 mL ethanolic solution of BHT (4.2%),

followed by mixing for 1 min by vortex. The mix was shaken for 15 min and then centrifuged for 5 min at 6000 rpm. The supernatant was filtered with Whatman No. 1 filter paper. The filtrate (4 mL) was mixed with 4 mL of TBA (0.02 mol/L) and heated in a water bath (100 °C) for 45 min. The measurements were recorded after cooling and filtering at 538 nm using an ultraviolet spectrophotometer (Cecil CE 1021, Cambridge, United Kingdom). The values of TBARS were expressed as mg malondialdehyde (MDA)/kg of sample.

3.5.13.3 Color analysis

Colorimetric analysis of the dispersion samples was conducted using an UltraScan VIS spectrophotometer (Hunter Associates Laboratory, Inc., Reston, VA, USA) operated in total transmission mode. Prior to the measurement of colour parameters for the meat samples, the instrument was calibrated against a white standard plate. The spectrophotometer was configured according to the CIE La*b* colour space. As the combination of a* and b* provides a more comprehensive representation of colour, the hue angle (in degrees) and chroma were calculated using the standard formulae (Lapčík et al. 2025):

$$h^* = \arctan \frac{a^*}{b^*} \tag{9}$$

$$C^* = \sqrt{(a^*)^2 + (b^*)^2} \tag{10}$$

3.5.14 Statistical Analysis

All the experiment results were analysed using one-way ANOVA with Duncan's multiple-range test. Differences in the mean values among statistical groups were tested at a significance level of $\alpha \leq 0.05$. Sigma plot, version 12.5(Systat Software, San Jose, CA, USA) was used for data analysis, Origin Pro (OriginLab, Northampton, MA, USA) for curve normalisation and Design

Expert (Stat-Ease Inc., Minneapolis, MN, USA) for designing the experiment and analysis of the model created.

3.5.15 Integrated Evaluation of the Functional Properties of Films (IFE)

Multivariate analysis on the standardisation of experimental data was performed. The parameters considered were water vapour permeability, mechanical properties (TS, EB and EM), antioxidant activity (at 4° and 25 °C), microbial, peroxide value and TBARS analysis of minced chicken and beef. Each variable was normalised using the min-max method as:

$$x_{norm} = \frac{(x - x_{min})}{(x_{max} - x_{\min})} \quad (11)$$

where x is the observed value, x_{min} is the minimum observed value, and x_{max} is the maximum observed value. Following this, the functional index for active packaging was calculated using the following equation:

$$IFE = \frac{1}{n} \sum_{i=1}^{n} x_{norm} \quad (12)$$

Pearson's correlation analysis was carried out among the parameters chosen to investigate the potential relationships between structure and functionality.

4 Results and discussion

4.1 Results and discussion of individual experiments

4.1.1 Experiment I, II, and III

Experiments I, II, and III were primarily conducted to develop the DOE and to formulate the bioactive films. Subsequently, the films were evaluated for their mechanical properties and swelling ratio. The regression equations were derived with R^2 values of 0.90 for tensile strength, 0.86 for elasticity, 0.83 for strain, and 0.99 for swelling ratio. The R^2 values confirmed the accuracy and reliability of the modelled relationships. The corresponding three-dimensional response surface plots are presented in Fig. 1.

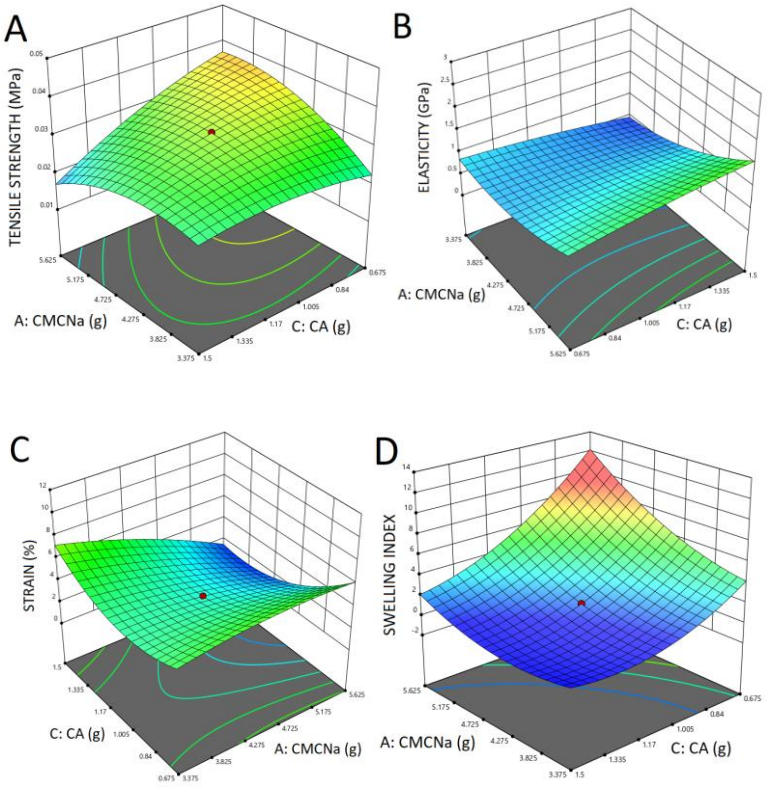

Fig.1: Response Surface Plots showing the relation between the concentration of CMCNa and CA on the selected film analyses: tensile strength (A), elasticity (B), strain (C) and swelling index (D).

4.2 Results and discussion of selected experiments

4.2.1 Scanning Electron Microscopy and Confocal Scanning Microscopy

The morphological features of the film samples examined using SEM and CLSM are presented in Figures 2 and 3, respectively.

The SEM analysis revealed a comparatively smooth surface in the control film, while films incorporating essential oils displayed marked surface heterogeneity. Spherical droplets of various sizes were observed to be dispersed throughout the polymer matrix, indicating successful encapsulation. The encapsulated structures appeared well-defined, suggesting that the encapsulation process was effective and did not compromise the structural integrity of the polymer network.

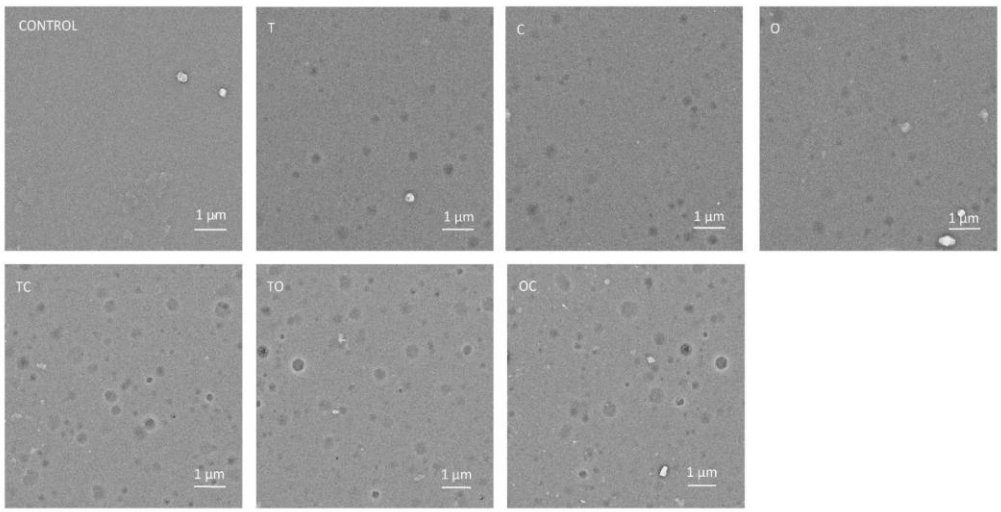

Fig.2: SEM images of the film samples.

The encapsulation of EOs was strongly supported by the CLSM imaging. The distribution of the oil was visible throughout the film. Furthermore, the encapsulated oils had a thicker outer coating, which could be

associated with forming a porous cellulose hydrogel shell around the oil (Hamal et al. 2022).

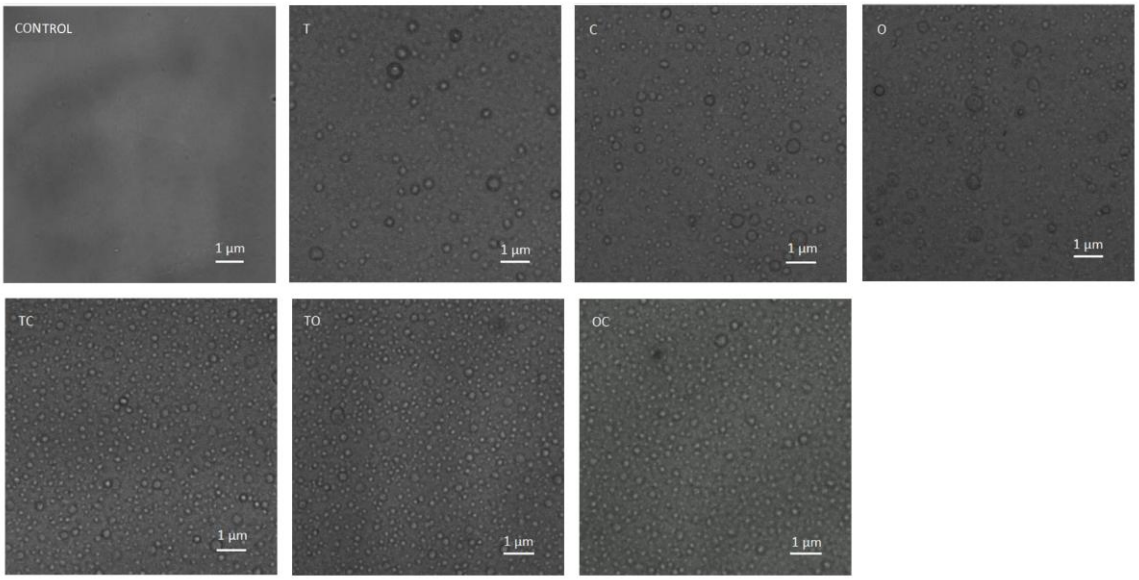

Fig. 3: CLSM images of the film samples.

4.2.2 Light transmittance and opacity

The results of film thickness, transparency, and moisture content are given in Table 2, followed by the light transmittance data in Table 3. The visual representation of the films is given in Fig. 4. The thickness of the films ranged from 0.08 mm to 0.1 mm with no significant difference ($p < 0.05$). The films were highly transparent. From the food quality assessment context, high transparency is desirable for food packaging. A higher transparency value corresponds to a lower UV barrier property. In the presented study, all the film samples with EOs had better UV barrier properties than the control sample. Additionally, the films with two EOs had better UV barrier properties than those with one EO. This observation was consistent with the works of Gautam, Lapcik et al. (2023).

Table 2: Results of thickness, transparency and moisture content. Differences in the mean values among the statistical groups were tested at a significance level of $p < 0.05$. The results are expressed as arithmetic mean ± standard deviation.

Sample	Thickness (mm)	Transparency	Moisture Content (%)
CON	0.08 ± 0.001^{a}	0.52 ± 0.03^{a}	0.04 ± 0.03^{a}
T	0.10 ± 0.001^{a}	1.79 ± 0.02^{b}	0.12 ± 0.13^{b}
C	0.08 ± 0.001^{a}	1.36 ± 0.04^{ab}	0.14 ± 0.13^{b}
O	0.08 ± 0.001^{a}	1.36 ± 0.03^{ab}	0.10 ± 0.1^{b}
TC	0.08 ± 0.001^{a}	1.35 ± 0.24^{ab}	0.06 ± 0.06^{c}
TO	0.09 ± 0.001^{a}	1.09 ± 0.02^{a}	0.03 ± 0.01^{a}
OC	0.09 ± 0.001^{a}	1.19 ± 0.06^{ab}	0.10 ± 0.08^{b}

Table 3: Light transmittance values at various wavelengths of the prepared samples. Differences in the mean values among the statistical groups were tested at a significance level of $p < 0.05$. The results are expressed as arithmetic mean ± standard deviation.

Sample	Light transmittance %						
	280	**350**	**400**	**500**	**600**	**700**	**800**
CON	24.05 ± 2.28^{a}	77.59 ± 0.72^{a}	83.38 ± 1.92^{a}	87.57 ± 0.62^{a}	88.72 ± 0.61^{a}	88.17 ± 0.42^{a}	88.92 ± 0.89^{a}
T	$0.51 \pm^{*} 0.11^{b}$	36.48 ± 0.92^{b}	47.3 ± 0.85^{b}	59.12 ± 1.01^{b}	66.17 ± 0.32^{b}	72.86 ± 3.31^{a}	74.25 ± 0.77^{b}
C	1.10 ± 0.6^{ab}	41.73 ± 2.38^{c}	57.10 ± 2.46^{c}	67 ± 1.48^{c}	73.17 ± 0.68^{ab}	75.23 ± 1.06^{a}	77.75 ± 0.85^{ab}
O	1.10 ± 0.15^{ab}	45.85 ± 0.49^{c}	56.67 ± 0.49^{c}	65.83 ± 1.85^{c}	73.12 ± 0.51^{ab}	75.92 ± 0.4^{a}	79.81 ± 1.39^{ab}
TC	6.99 ± 1.03^{a}	53.56 ± 3.22^{d}	59.5 ± 2.9^{d}	69.29 ± 3.4^{d}	73.31 ± 4.05^{ab}	74.71 ± 3.88^{a}	76.17 ± 4.29^{ab}
TO	3.41 ± 0.28^{ab}	54.16 ± 0.81^{d}	63.78 ± 0.75^{cd}	73.35 ± 1.24^{cd}	77.88 ± 0.34^{a}	80.97 ± 0.39^{a}	83.11 ± 0.11^{ab}

OC	1.87 ± 0.50^{ab}	50.19 ± 2.16^{cd}	62.31 ± 2.25^{cd}	71.07 ± 1.16^{cd}	76.04 ± 1.07^{ab}	78.95 ± 0.64^{a}	81.98 ± 1.37^{ab}

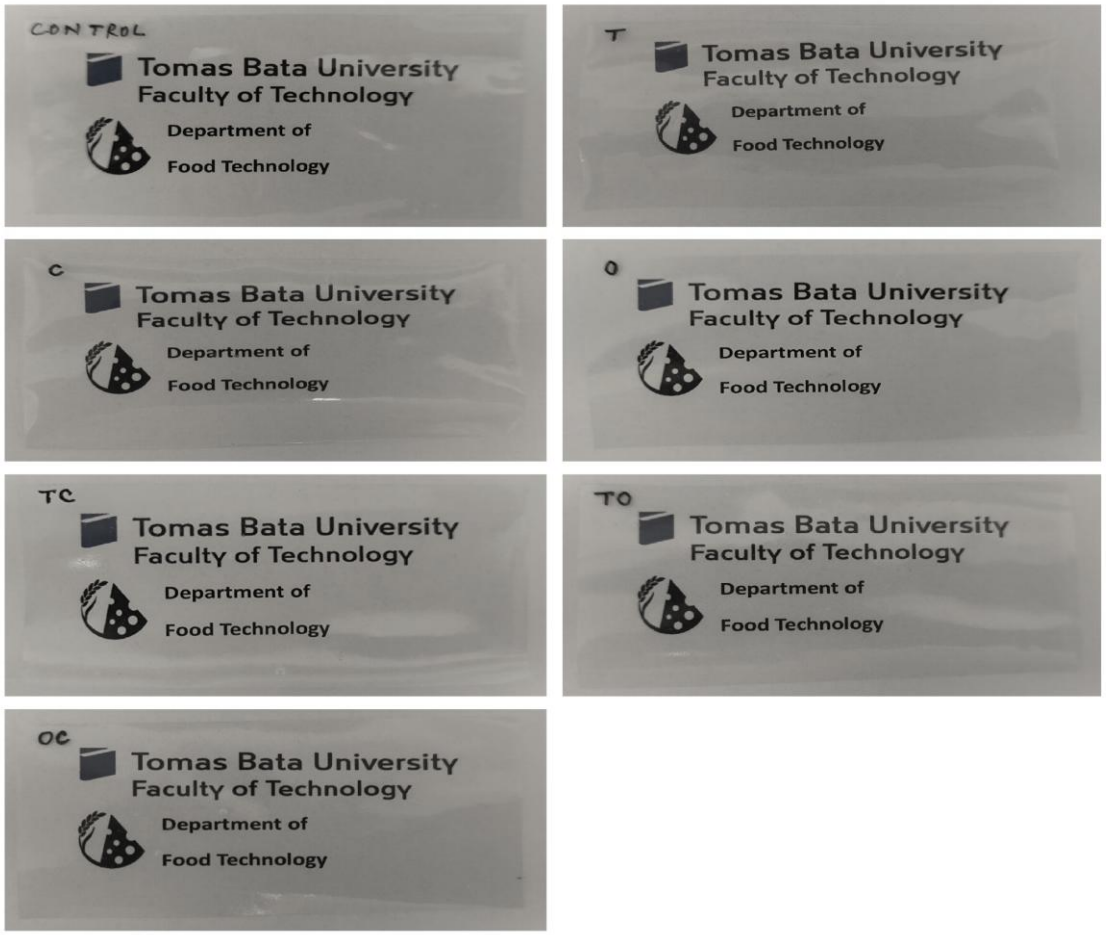

Fig. 4: Visual appearance of the films.

4.2.3 Antioxidant activity

The results of the antioxidant activity are presented in Figs. 5 and 6. At 25 °C in DW, all film samples exhibited a general increase in antioxidant activity, reaching a maximum at 10 hours, followed by a subsequent decline at 48 hours. In 3% acetic acid, the antioxidant activity gradually increased, peaking at 6 hours, after which a steady decrease was observed, culminating in a significant reduction by 48 hours. In 10% EtOH, a gradual increase in antioxidant activity was recorded, with a peak at 10 hours, and only a slight, statistically insignificant decline was noted up to 48 hours. In 50% EtOH, the

antioxidant activity increased and peaked at 6 hours, followed by minor fluctuations without significant changes throughout the 48-hour period.

At 4 °C, the films in DW exhibited relatively consistent antioxidant activity over the 48-hour period, with only minor, statistically insignificant fluctuations. In 30% acetic acid, the antioxidant activity of the films declined gradually, reaching a dip at 8 hours, followed by a slow recovery to approximately the initial value by 48 hours. In 10% EtOH, the antioxidant activity remained largely stable, with no significant variation observed; however, a pronounced peak at 24 hours was detected for samples T, TC, OC, and C, which was subsequently followed by a notable decrease at 48 hours. In 50% EtOH, a sharp increase in antioxidant activity was observed at 4 hours and remained relatively stable thereafter, with a secondary peak at 12 hours observed specifically for sample C. In contrast, all other samples remained consistent before showing a significant decline in antioxidant activity at 48 hours from their respective peak values.

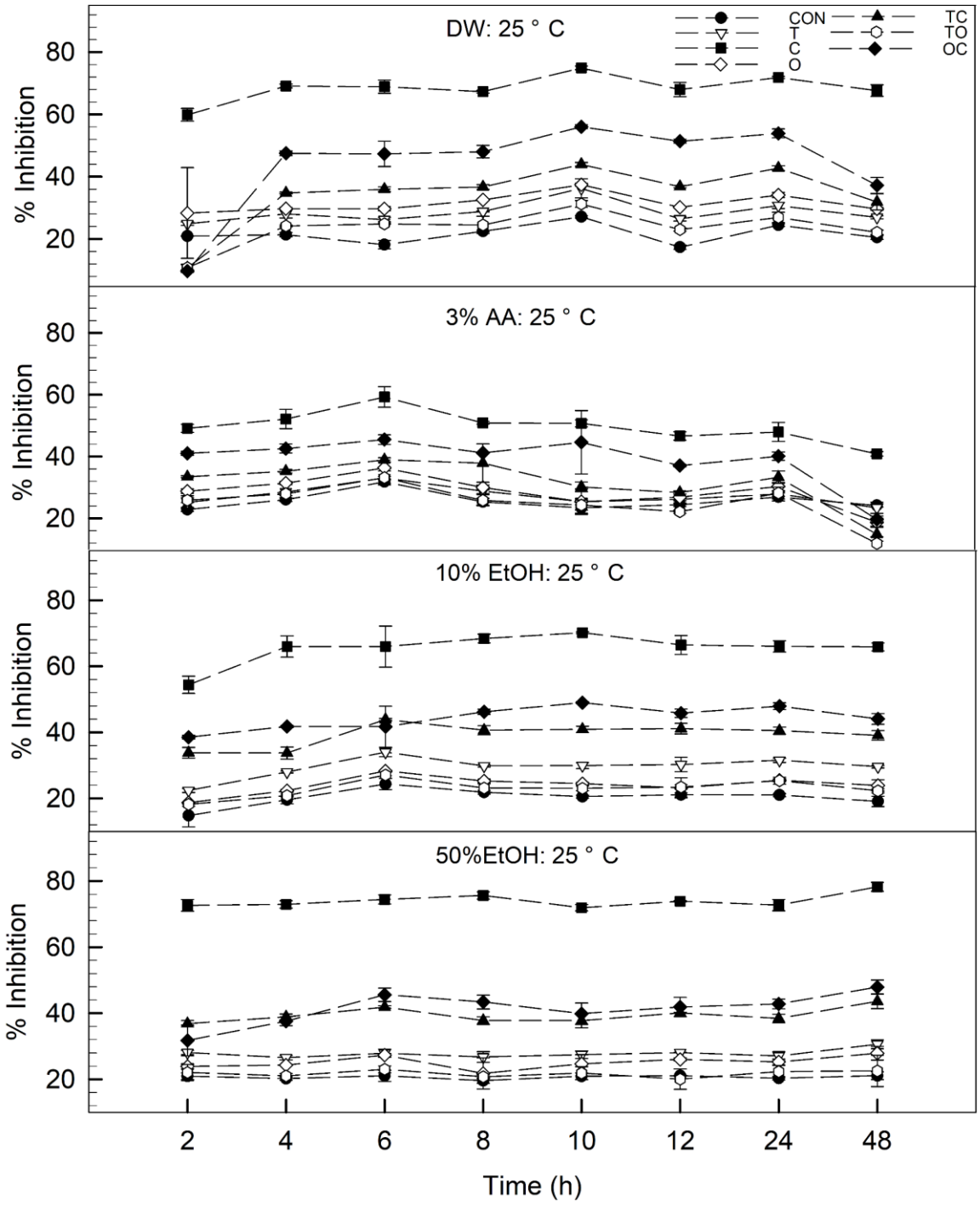

Fig. 5: Radical scavenging activity measured by DPPH, expressed as per cent inhibition in four food simulants at 25 °C.

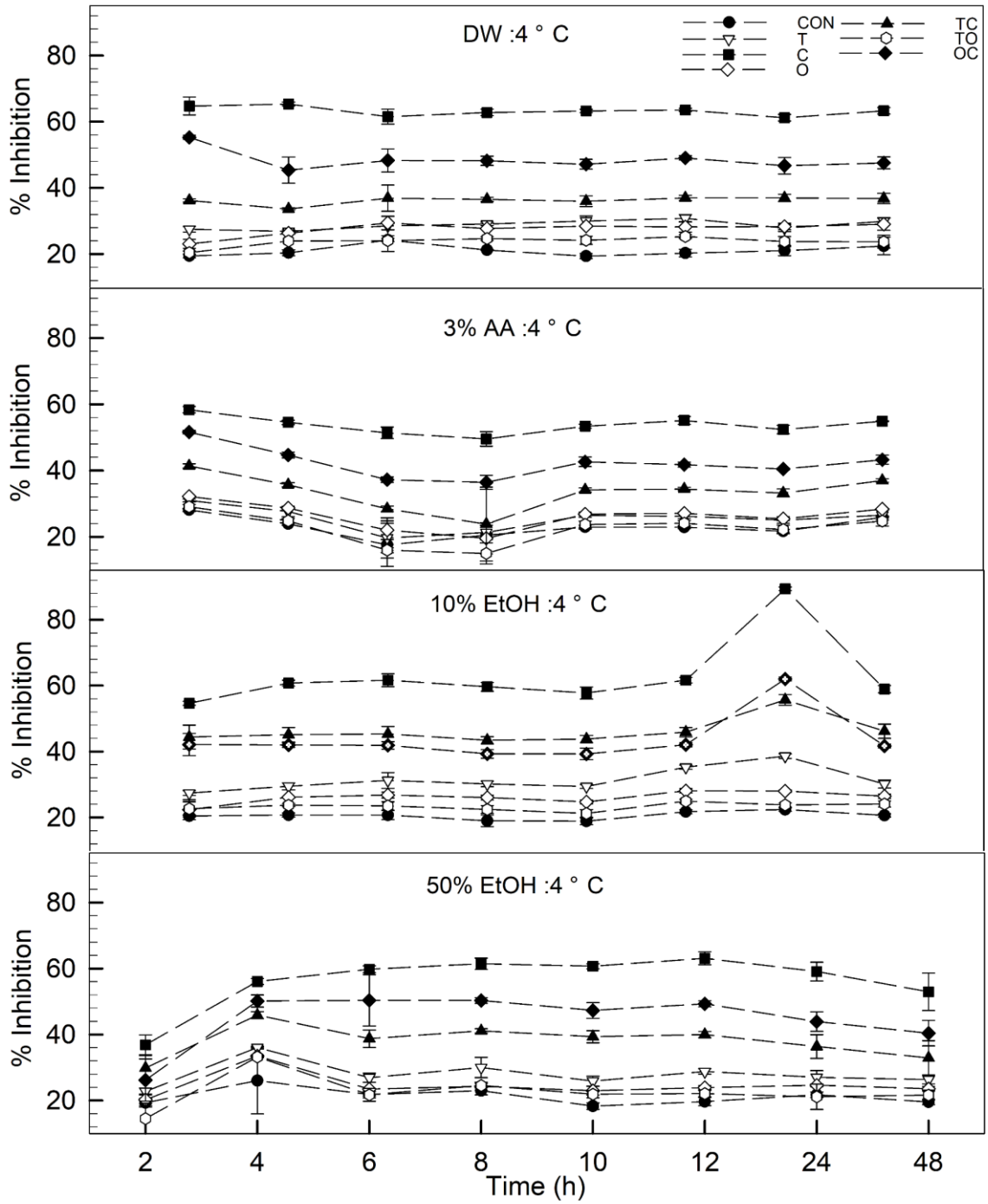

Fig. 6: Radical scavenging activity measured by DPPH, expressed as per cent inhibition in four food simulants at 4 °C.

4.2.4 Mechanical testing

The results of the mechanical testing are shown in Fig. 7. The tensile strength of the bioactive film samples was found to be either comparable to or higher than that of the control. The increased tensile strength in the bioactive films may be attributed to potential crosslinking interactions between the essential oils and the polymer matrix (Simsek et al. 2020). However, the overall tensile strength values were lower than those typically reported in the literature, which may be explained by the formation of rigid covalent bonds between citric acid and the carboxylate (COO^-) and sodium (Na^+) ions. This phenomenon was clearly reflected in the elasticity and strain results obtained in this study. Additionally, elastic modulus (EM), which reflects the toughness of the films and their ability to withstand deformation under pressure, was highest in the control sample. These findings were in agreement with the results reported by Gautam, Lapcik et al. (2023).

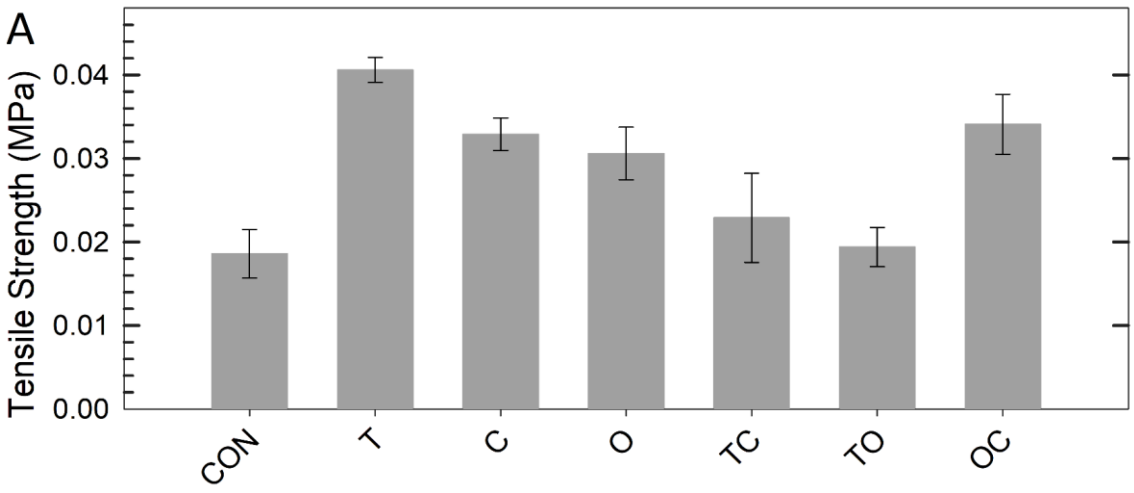

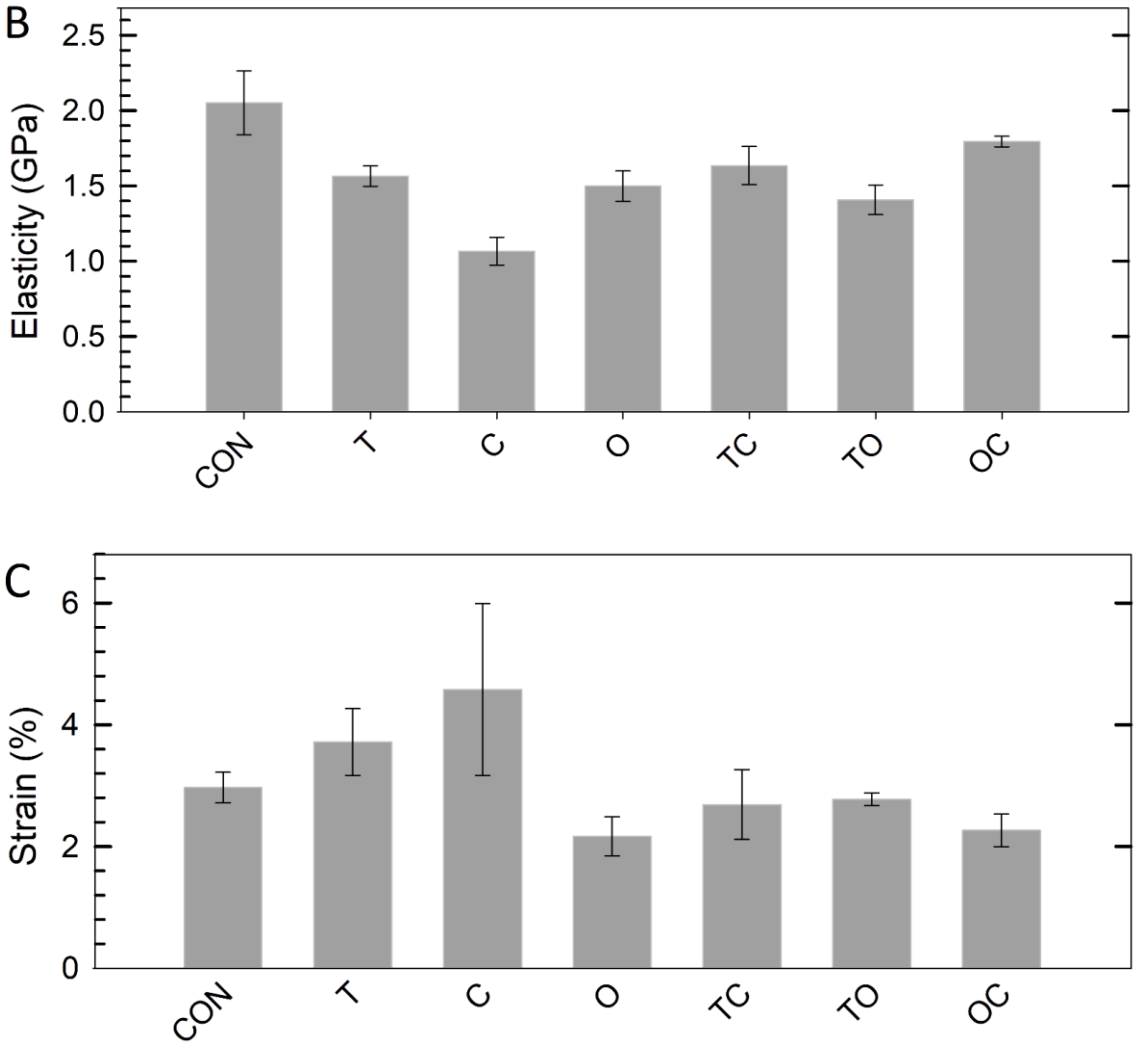

Fig. 7: Mechanical testing (A: tensile strength, B: elasticity and C: strain) of the film samples. Differences in the mean values among the statistical groups were tested at a significance level of $p < 0.05$.

4.2.5 Moisture Absorption Kinetics

The results of the moisture content analysis are presented in Table 2, while the rate of moisture absorption, measured at a relative humidity of 97%, is shown in Fig. 8. The moisture content of the films ranged from 4.7% to 5.5% by weight, with no statistically significant differences observed ($p < 0.05$). These values were lower than those typically reported in the literature, which may be attributed to the crosslinking process - a heat-mediated dehydration reaction.

The rate of moisture absorption exhibited a relatively non-uniform trend. Sample C demonstrated the highest rate of moisture absorption, followed by samples T<OC<O<TC<CON<TO. The elevated absorption rates observed in samples C, T, O, and OC may be attributed to the sparingly soluble nature of the incorporated EOs. Furthermore, samples T, C, and OC displayed higher values of both moisture absorption equilibrium (c_0) and the rate constant (k), indicating their capacity to absorb substantial amounts of moisture at a rapid rate (Fig. 9). Conversely, samples CON, TC, and TO exhibited lower c_0 values but relatively higher k values, suggesting the ability to absorb smaller quantities of moisture quickly - characteristic of materials with low porosity and a hydrophilic surface. Notably, sample O deviated from this pattern, presenting a high c_0 value alongside a low k value, which implies a slower uptake of a larger quantity of moisture and is indicative of a denser polymer matrix.

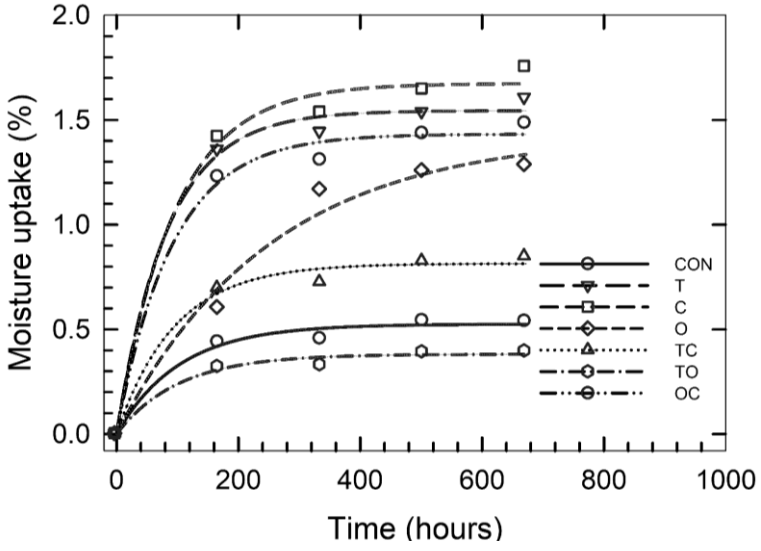

Fig. 8: Rate of moisture absorption by the film samples.

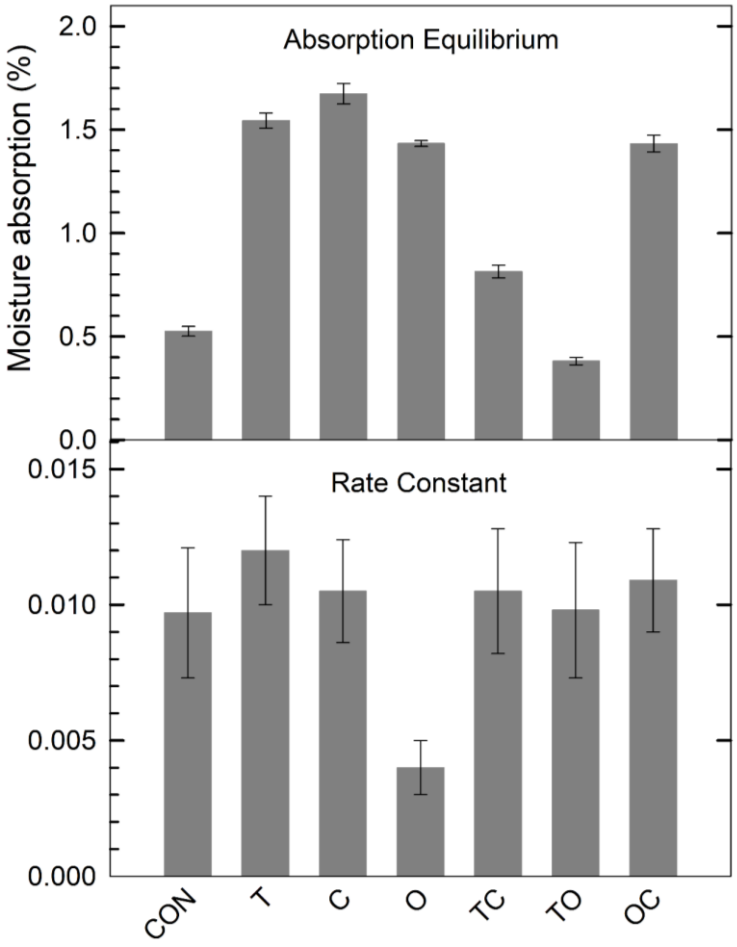

Fig. 9: Moisture absorption equilibrium and rate constant of the film samples.

4.2.6 Water Vapor Permeability-Water vapor Transmission Rate

The water vapour permeability (WVP) and water vapour transmission rate (WVTR) of the films under investigation are presented in Fig. 10. It was found that permeability was not significantly influenced by the presence or specific type of bioactive substances ($p < 0.05$). This absence of statistical significance may be attributed to the uniform composition of the polymer matrix, suggesting that the transport properties are predominantly governed by a diffusion-controlled mechanism. The WVP values were consistently similar across all film samples, in marked contrast to the variations observed in the moisture absorption study.

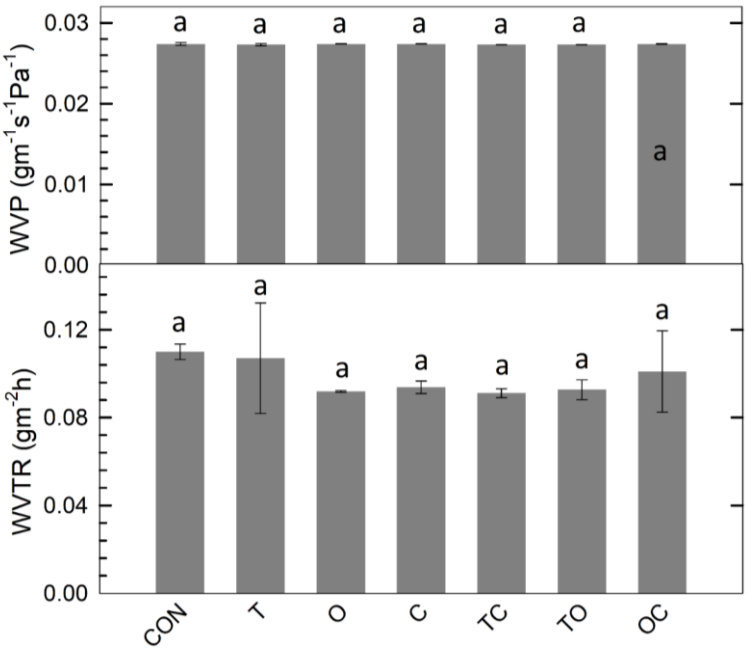

Fig. 10: WVP and WVTR of the film samples. Differences in the mean values among the statistical groups were tested at a significance level of $p < 0.05$.

4.2.7 Swelling ratio

The swelling behaviour of the bioactive films is illustrated in Fig. 11. The presence and combination of EOs were found to influence the swelling characteristics of the films. The control sample exhibited a moderate swelling ratio of 4.83 ± 0.32 g. Films containing individual oils demonstrated lower swelling ratios (ranging from 2.2 to 2.4 g), which may be attributed to the hydrophobic nature of the oils, resulting in reduced interaction between the film matrix and water molecules (Gautam, Lapcik et al. 2023, Valderrama Solano, de Rojas Gante 2012). Sample TC exhibited an anomalously high swelling ratio of 7.07 ± 0.78 g. This deviation may be explained by a disruption of the polymeric network, potentially caused by poor compatibility or phase separation between the two oils, thereby creating microdomains that facilitate water ingress (Mouhoub et al. 2023). In contrast, samples TO and OC displayed moderate swelling behaviour. This effect may be linked to interference with polymer–crosslinker interactions and/or alterations in the porosity of the polymer network.

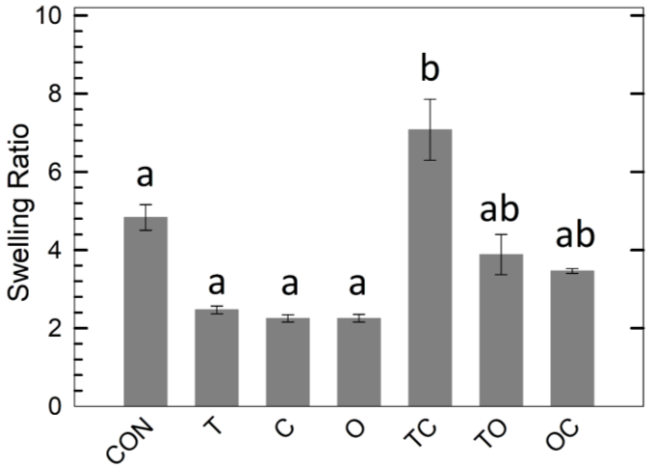

Fig. 11: Swelling index of the film samples. Differences in the mean values among the statistical groups were tested at a significance level of $p < 0.05$.

4.2.8 Gel Fraction

The results of the gel fraction analysis are presented in Fig. 12. This analysis was performed to evaluate the extent of crosslinking between the cellulose-based polymers and the crosslinking agent. All film samples exhibited a gel fraction exceeding 99%, clearly suggesting successful crosslinking. Samples T and C showed significantly lower values compared to the control, which may be attributed to the sparingly soluble nature of thyme and clove essential oils (Gautam, Lapcik et al. 2023), potentially leading to minor alterations in the polymer matrix.

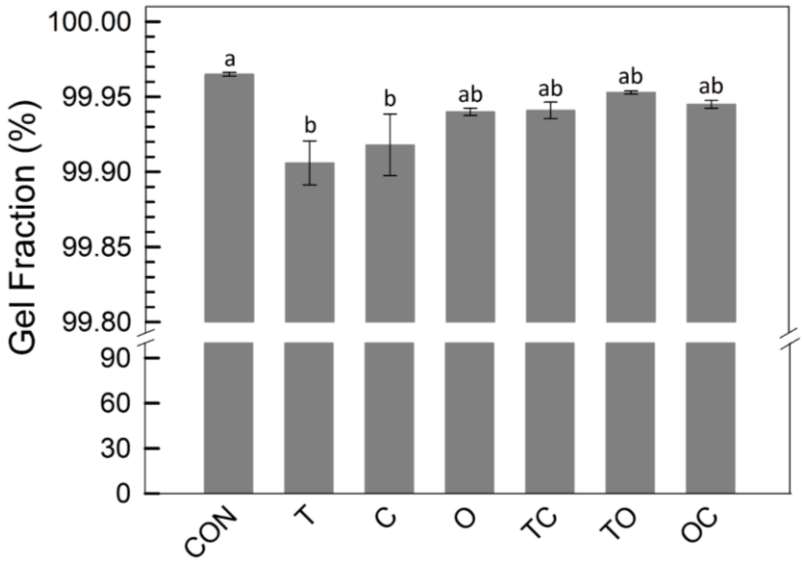

Fig. 12: Gel fraction of the film samples. Differences in the mean values among the statistical groups were tested at a significance level of $p < 0.05$.

4.2.9 Thermogravimetric analysis

The results of the thermogravimetric analysis are presented in Fig. 13. Three major thermal events, corresponding to weight loss, were observed across all samples. The first event occurred within the temperature range of 30–200 °C and was attributed to the evaporation of moisture and the loss of volatile compounds, resulting in an 8–12% reduction in mass. The second significant weight-loss event was recorded between 200–400 °C, leading to a reduction of 55–56% in sample mass. Similar trends were documented by Sotolářová et al. (2021) in HEC films crosslinked with citric acid. The sharp decline in mass observed beyond 230 °C has been associated with the thermal degradation of carboxylate (COO^-) groups present in CMCNa. The final event, occurring between 400–600 °C, corresponded to the complete decomposition of the films. No appreciable differences were observed between the bioactive and control samples.

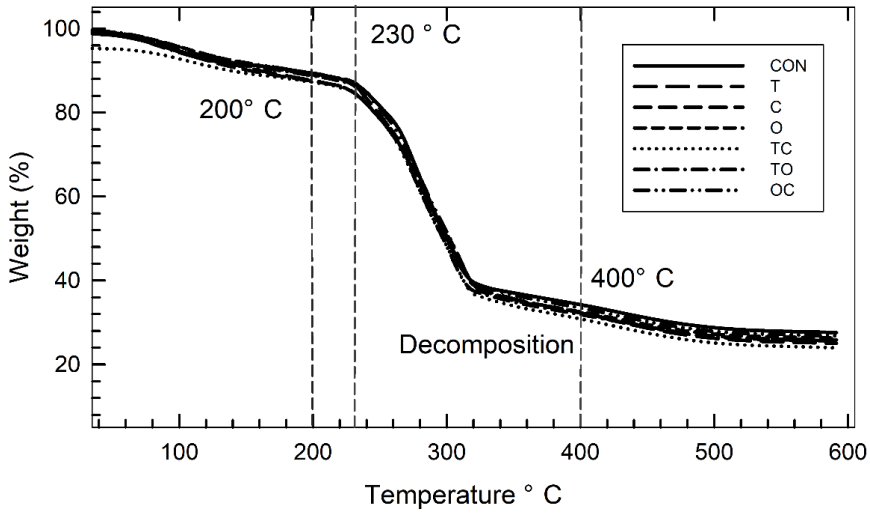

Fig. 13: Thermogravimetric analysis of the film samples.

4.2.10 Fourier Transform Infrared Spectroscopy

ATR-FTIR spectroscopy was employed to investigate the interactions among CMCNa, EOs, and CA. The corresponding spectra are presented in Figs. 28 and 29. Overall, the films exhibited similar spectral profiles, with variations primarily observed in peak intensities. Prominent absorption bands were noted within the 3000–3500 cm^{-1} region, corresponding to O–H stretching vibrations of CMCNa. Peaks within the 1000–1500 cm^{-1} range were attributed to asymmetric and symmetric stretching of carboxylate (COO^{-}) groups. A distinct band observed at 1589 cm^{-1} was ascribed to the C=O stretching vibrations characteristic of cellulose (Ghorpade et al. 2019). Additionally, bands at 2967 cm^{-1} and 1025 cm^{-1} were associated with C=O groups derived from glycerol. A minor shoulder at 1704 cm^{-1} was also identified and attributed to the carboxylic group stretching mode of glycerol, consistent with earlier findings (Danish et al. 2017).

For the bioactive films, differential spectra relative to the control sample were calculated and are illustrated in Fig. 29. The principal bioactive constituents identified included thymol, carvacrol, *p*-cymene, eugenol, and

their respective derivatives. A broad absorption band in the 3200–3300 cm^{-1} region was attributed to the stretching vibrations of hydrogen-bonded –OH groups, commonly present in hydration water as well as in alcohol and phenolic compounds (Catauro et al. 2017). Characteristic peaks observed at 804 cm^{-1} and 811 cm^{-1} were associated with thymol and carvacrol, respectively (Topala, Tataru 2016), while peaks at 1767 cm^{-1} and within the 1100–1210 cm^{-1} region corresponded to eugenol acetate and the C–O–C stretching vibrations of eugenol (Gao et al. 2017).

Peaks attributed to thymol were detected between 841–862 cm^{-1} (samples T, O, and TO), while signals corresponding to terpinene appeared within the 902–928 cm^{-1} region (also in samples T, O, and TO). Peaks within the 1500–1600 cm^{-1} range, detected in samples containing thyme and oregano essential oils, were ascribed to the C–H stretching vibrations of benzene rings and/or C=C stretching of aromatic carbon double bonds. Bands observed between 1100–1500 cm^{-1} were attributed to various bending and stretching modes, and the out-of-plane O–H bending vibrations were noted within the 736–590 cm^{-1} region (Catauro et al. 2017). Notably, a peak at 1495 cm^{-1}, identified in samples C, TC, and OC, was attributed to the C–H deformation vibration of the eugenol methyl group.

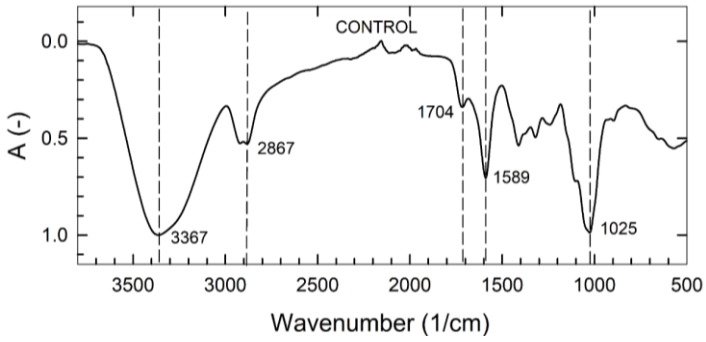

Fig. 14: FTIR spectrum for the control sample with major peaks.

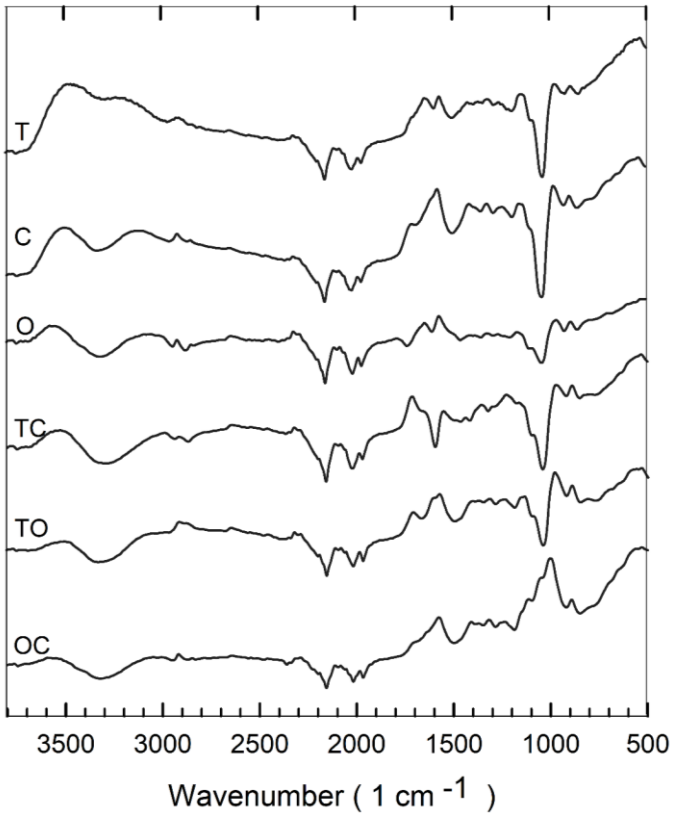

Fig. 15: FTIR differential spectrum for bioactive film samples calculated relative to the control sample.

4.2.11 Biodegradability in soil

The results of the film biodegradation study are depicted in Fig. 30. No distinct degradation pattern was discernible among the different samples. The percentage of weight loss exhibited significant variation across the films ($p > 0.05$). However, it was observed that the control sample experienced a comparatively higher degree of weight loss than the bioactive films. This outcome may be attributed to the hydrophobic characteristics of the essential oils, which may have hindered the penetration of moisture and microbial activity, thereby decelerating the degradation process. Despite this variation, complete degradation was achieved for all film samples by the end of the second week.

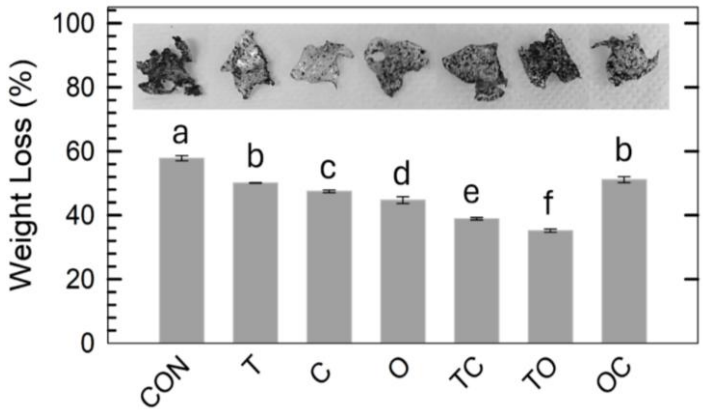

Fig. 16: Biodegradability as a function of weight loss for the film samples. Differences in the mean values among the statistical groups were tested at a significance level of $p < 0.05$.

4.2.12 Microbiology analysis

The results of the antimicrobial activity assessment are presented in Table 4 and Fig. 17. The films exhibited inhibitory effects against Gram-negative bacteria, whereas no significant activity was observed against Gram-positive strains. Although the EOs employed in this study have previously been reported to demonstrate high efficacy against both *E. coli* and *S. aureus*, it is presumed that the concentration of oils incorporated into the films was insufficient to exert a measurable effect against *S. aureus*. Film sample C exhibited the largest inhibition zone (6.2 ± 0.13 mm).

Table 4: Antibacterial property of the films determined by agar disc diffusion assay. Differences in the mean values among the statistical groups were tested at a significance level of $p < 0.05$. The results are expressed as arithmetic mean ± standard deviation.

Sample	**Antibacterial activity (mm)**
CON	2.2 ± 0.08^{a}
T	5.6 ± 0.11^{b}

C	6.2 ± 0.13^{b}
O	4.8 ± 0.13^{b}
TC	5.4 ± 0.09^{b}
TO	4.6 ± 0.16^{ab}
OC	5.2 ± 0.13^{b}

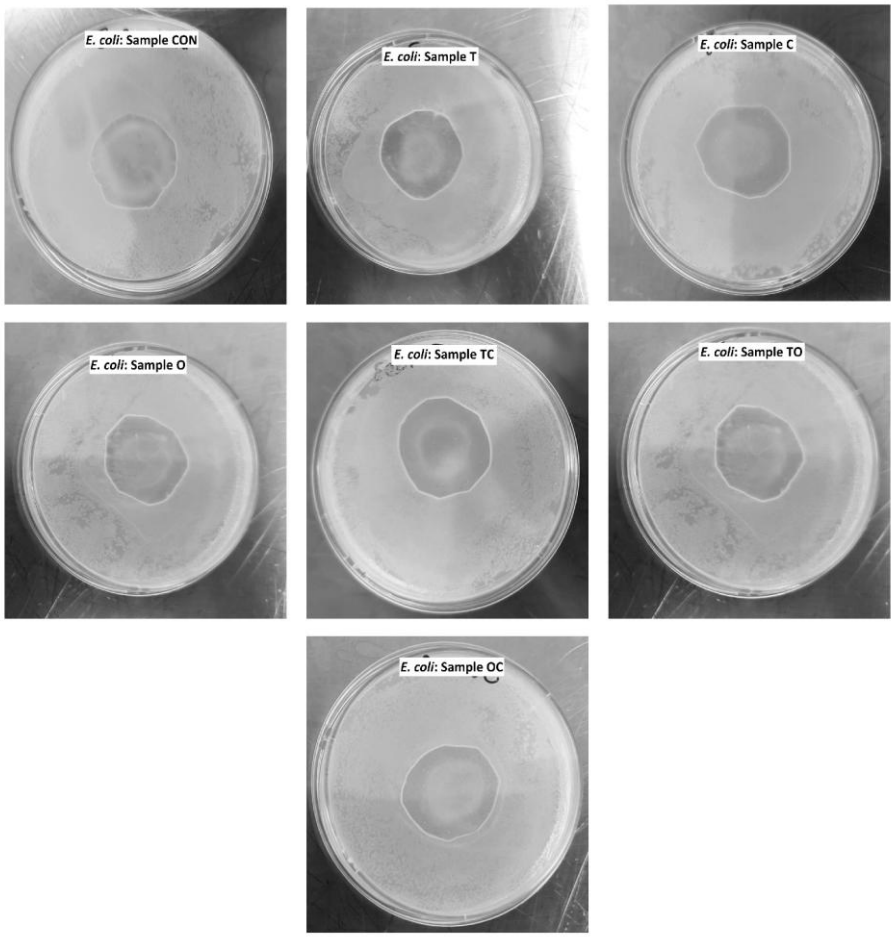

Fig. 17: Representative pictures of inhibitory zones of the film samples against E. coli.

4.2.13 Shelf-Life study

The criteria for selecting a suitable food model were grounded in literature and aligned with the practical demands of preserving perishable, high-moisture food matrices like ground chicken and beef. The criteria were qualitatively defined as follows:

- High crosslinking degree and low WVP: essential for ensuring moisture resistance and preventing film degradation in the humid environment of minced meat;
- Pronounced antioxidant activity: particularly relevant for controlling lipid oxidation processes typical in ground meat systems;
- Demonstrated antibacterial efficacy against Gram-negative bacteria: important for mitigating microbial growth during storage;
- Mechanical flexibility and integrity: enabling the films to adhere effectively to irregular meat surfaces without tearing or disintegrating;

These criteria collectively supported the selection of minced meat as a representative food model to evaluate the films' practical preservation efficiency under refrigerated conditions.

4.2.13.1 Microbial study

The results of the Total Psychrotrophic Count are illustrated in Fig. 18. The microbial load on day 0 indicated minimal initial contamination across all chicken meat samples. However, by day 4, a linear increase in psychrotrophic bacterial growth was observed in all samples, with the microbial load reaching ≈ 5 log CFU/mL. By day 6, a divergence in growth trends was evident. All samples exceeded the spoilage threshold of 7 log CFU/mL, with sample T exhibiting the highest bacterial count (9.3 log CFU/mL). Moderate antibacterial effects were observed in samples C and O.

The initial analysis conducted on day 0 indicated a low microbial load across all beef samples. However, a substantial increase in microbial counts was observed by day 2. The uncoated control sample (Control 1) exhibited significantly higher bacterial growth compared to all biopolymer-coated samples, including the secondary control (Control 2). By day 6, all

biopolymer-coated samples remained well below the established spoilage threshold. Among these, sample C demonstrated the most effective antimicrobial activity, with a final count of 4.47 log CFU/mL, followed by samples O and TC.

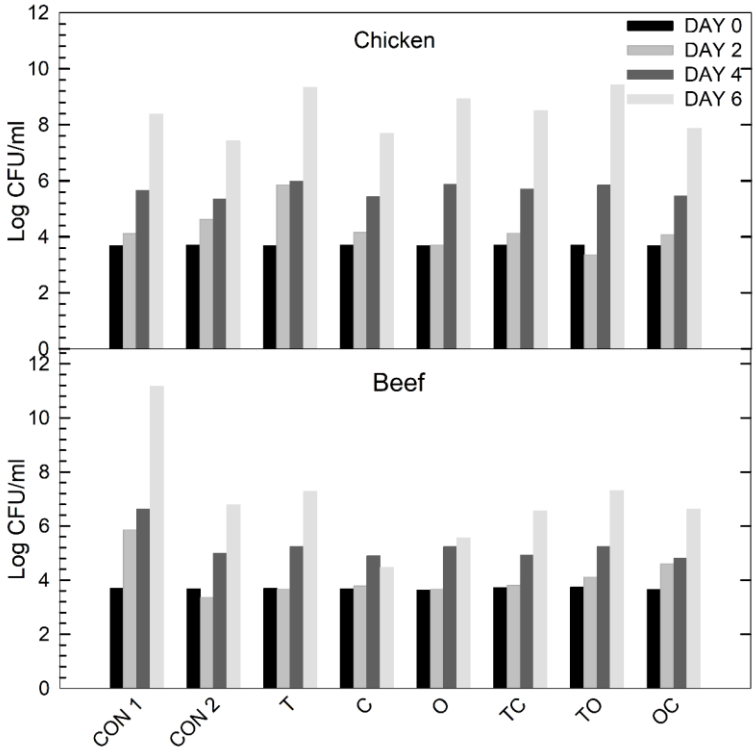

Fig. 18: Psychrotrophic bacteria count for the ground chicken and ground beef samples during 6-day storage at 4 ± 0.5 °C presented as Log CFU/mL.

4.2.13.2 Peroxide value analysis

The results of the peroxide value (PV) analysis are presented in Fig. 19. No consistent pattern was observed among the chicken samples. An increase in PV was recorded on day 2 for all samples except sample O, with the highest values observed for Control 1 and 2 (≈ 6 meq O_2/kg). Subsequently, the PV declined in all samples except C and O. This characteristic rise and fall in PV can be attributed to the oxidative degradation of unsaturated fatty acids.

For the beef samples, the PV increased and reached a peak on day 4 for all samples, except for samples O and TC, in which the peak was observed on day 2, followed by a decline on day 4. By day 6, a general decrease in PV was recorded across all samples, indicative of the anticipated degradation or exhaustion of primary oxidation products. Notably, samples O and TC deviated from this trend, maintaining elevated PV levels on day 6, which may suggest a continued formation of hydroperoxides or a delayed onset of secondary oxidation processes.

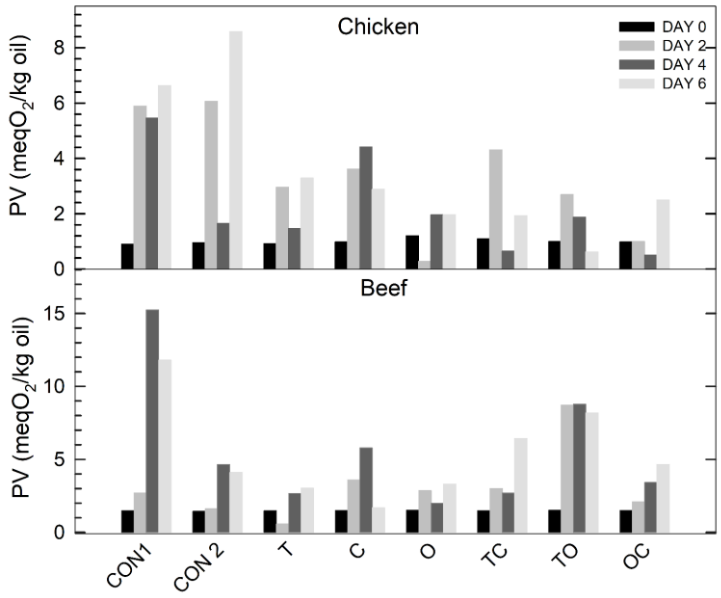

Fig. 19: Peroxide Value analysis for ground chicken and ground beef samples during 6-day storage at 4 ± 0.5 °C.

4.2.13.3 Thio barbituric acid analysis

The TBARS analysis results for both chicken and beef samples are presented in Fig. 20. In the case of ground chicken, the TBARS values on day 0 were comparable across all samples; however, from day 2 onwards, a statistically significant difference ($p < 0.05$) was observed between the control and the bioactive film-treated samples. By day 6, sample O demonstrated the most effective inhibition of secondary lipid oxidation, followed by sample TC.

Regarding ground beef samples, although the trend in malondialdehyde (MDA) formation mirrored that observed for chicken, superior antioxidative performance was exhibited by samples OC and O. It is recognised that ground meat is particularly prone to oxidative spoilage, leading to the generation of off-flavour compounds that compromise sensory acceptability. The threshold spoilage level for TBARS in both chicken and beef is 2 mg MDA/kg (Dalvandi et al. 2020, Soltana et al. 2024). Notably, none of the values in the current study reached this limit, and the findings for chicken agreed with the observations reported by Bishnoi et al. (2025).

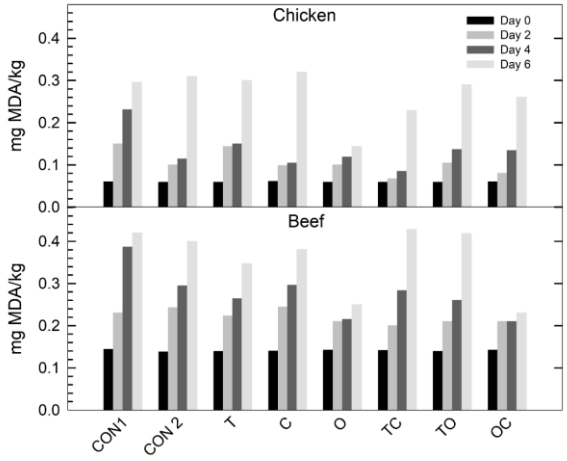

Fig. 20: TBARS analysis for ground chicken and ground beef samples during 6-day storage at 4 ± 0.5 °C.

4.2.13.4 Colour analysis

The packaged ground chicken and beef samples were monitored over 6 6-day storage period to assess the impact of bioactive films on the surface colour stability. The results are presented in Figs. 21 and 22 with their respective parameters (L*, a*, b*, Hue and Chroma).

For chicken samples coated in bioactive films, the L value (lightness) remained relatively stable from day 0 to day 6, indicating that the treatment did not significantly affect the brightness or darkness of the meat. In contrast,

a* value (redness) showed a significant reduction, suggesting the loss of red pigments was likely due to oxidative changes in the myoglobin. A corresponding decrease in b* values (yellowness) and a sharp reduction in chroma were also observed, indicating the overall loss of colour intensity and vividness. The hue angle increased significantly in all bioactive film samples, directing a perceptible shift from red to yellow hues. In sample CON 1, while the L* value remained unchanged, the a* value decreased significantly, the b* value remained relatively constant, the chroma decreased sharply (compared to the bioactive film samples), and the hue angle increased significantly, thereby reinforcing the general trend of myoglobin oxidation.

For beef samples, the L value remained relatively constant throughout the storage for all the samples, including CON 1. However, both a* and b* values decreased significantly, reflecting a pronounced loss in red and yellow tones, likely due to oxidative degeneration of oxymyoglobin. This was accompanied by a sharp reduction in colour saturation and vividness, typical for meat undergoing lipid and pigment oxidation. Moreover, there was also a significant increase in hue angle, further indicating a shift in colour from red to brownish tones. This can be further supported by the meat pigment oxidation processes.

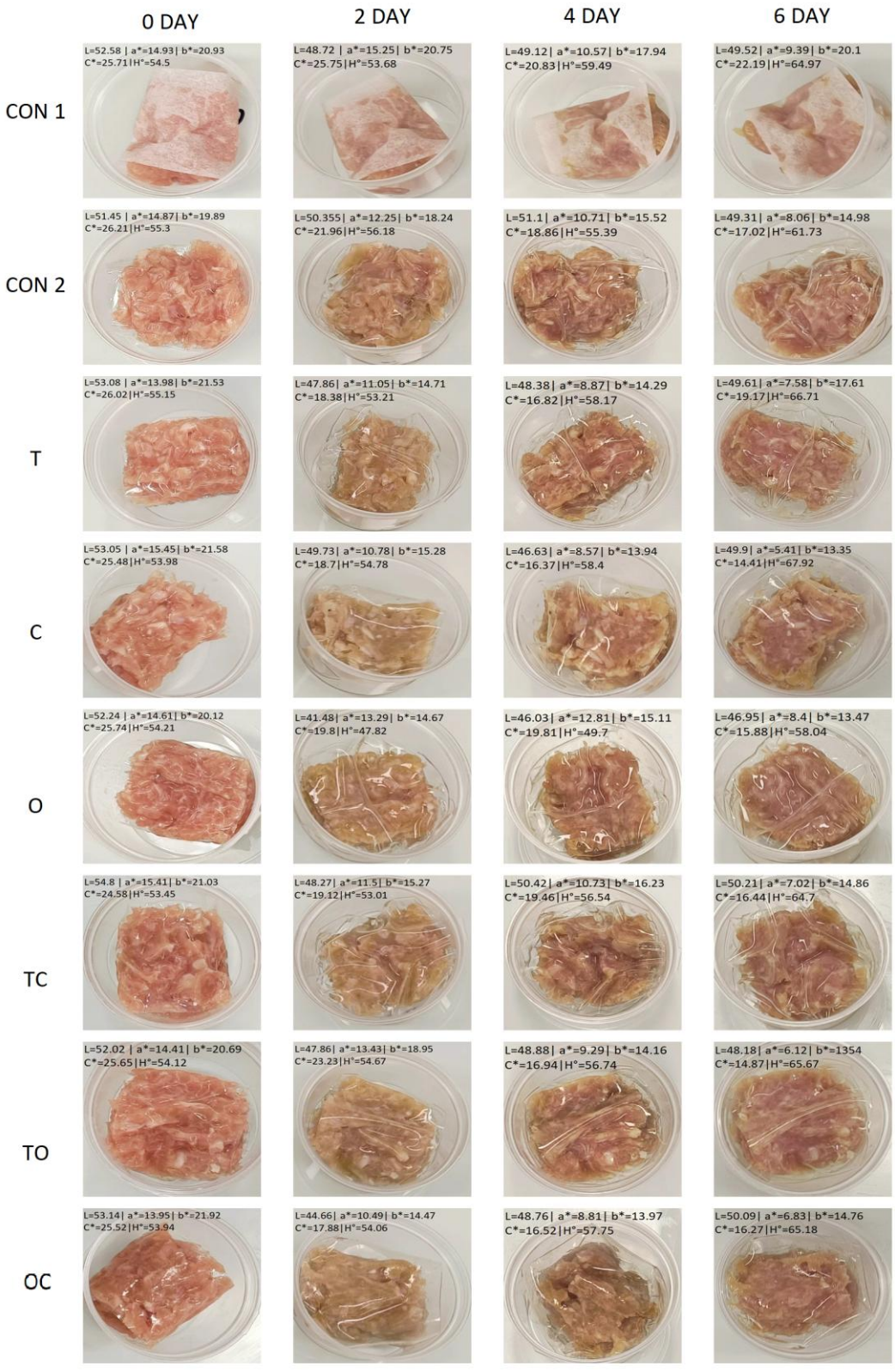

Fig. 36: Colour analysis of ground chicken samples during 6-day storage at 4 ± 0.5 °C.

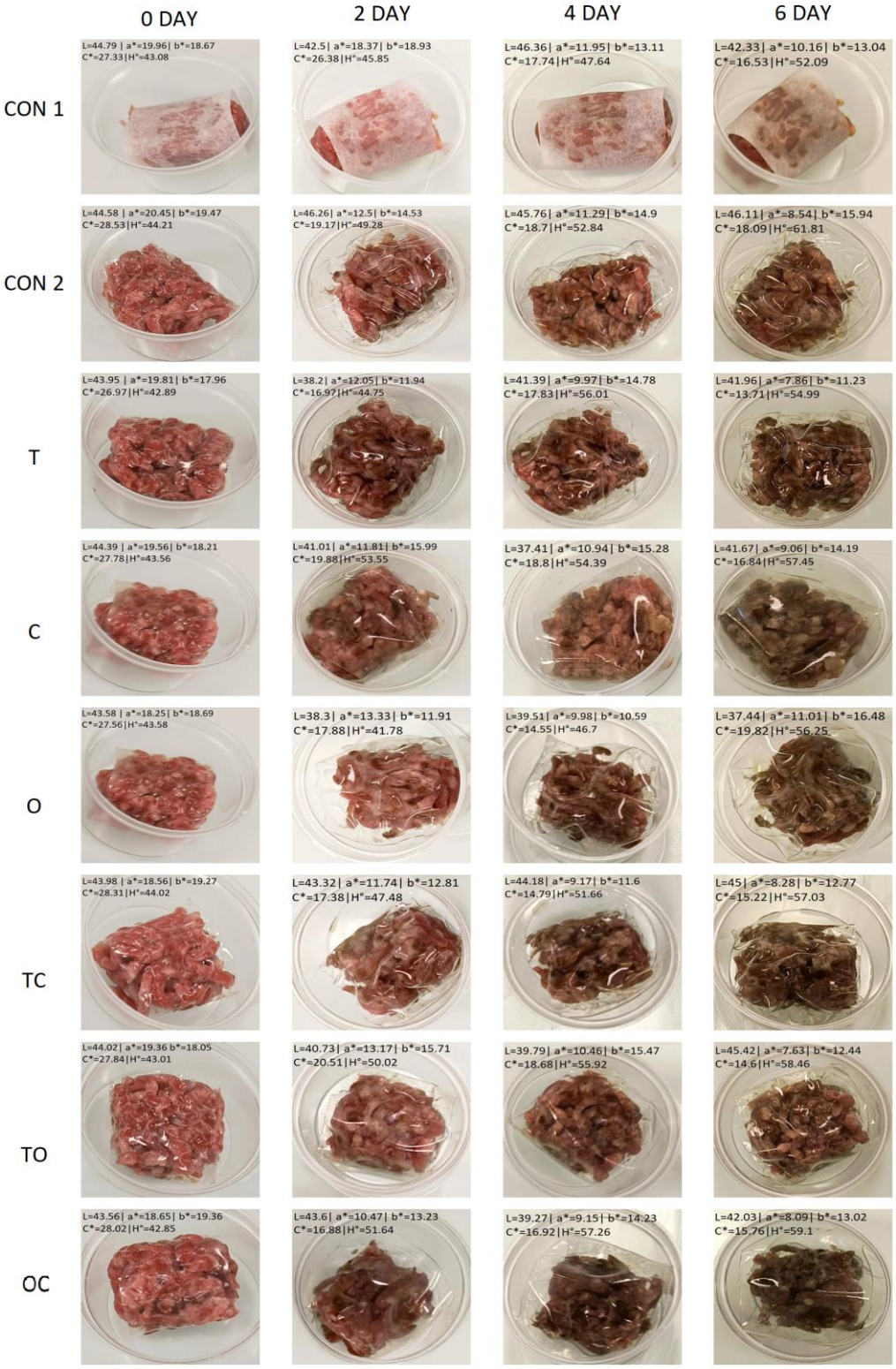

Fig. 37: Colour analysis of ground beef samples during 6-day storage at 4 ± 0.5 °C

4.2.14 Integrated Evaluation of the Functional Properties of Films (IFE)

The multivariate analysis was conducted in three sets. The first set aimed to evaluate the parameters related to the films, the second part, to evaluate the shelf-life parameters and the third one (holistic) was the combination of the two to uncover the best performing sample overall. The Pearson's correlation was conducted holistically to discover the impact of the films' parameters on the shelf-life parameters.

The IFE values for the samples are presented in Fig. 23. Sample C had the highest value (0.81), followed by sample OC (0.56) and TC (0.45). For the shelf-life parameters, the sample OC had the highest value (0.83), followed by samples O (0.61) and TC (0.59). The holistic IFE value was highest for sample C (0.68) and OC (0.65).

Pearson's correlation analysis revealed a moderately strong association between the antioxidant activity of the films (in all solvent systems) and the degree of microbial inhibition observed in beef samples. However, this relationship was weaker in chicken samples, likely due to their higher moisture content and rapid microbial proliferation. Additionally, a moderate correlation was observed between TBARS and peroxide values in beef, again, less pronounced in chicken. These findings align with previous microbiological and oxidative stability results, reinforcing the view that meat matrix composition plays a pivotal role in modulating the films' protective effects.

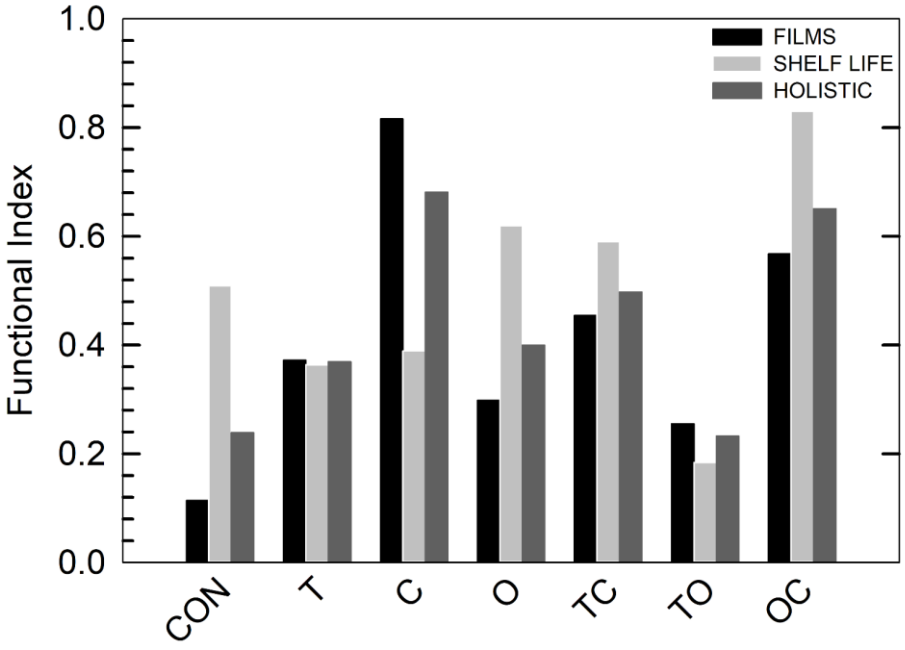

Fig. 23: Functional index of the film samples.

5 CONTRIBUTION TO SCIENCE AND PRACTICE

EOs are increasingly recognised as versatile and effective bioactive substances, widely valued for their potent antioxidant, antimicrobial, and nutritive properties. This research explores an eco-friendly solution aligned with the current demand for green technologies. The study's outcomes contribute to the scientific understanding of polymer-bioactive interactions and demonstrate practical relevance in food preservation systems. The specific contributions of this study to both scientific knowledge and real-world applications can be summarised as follows:

1. A systematic optimisation process was undertaken to identify a film composition that achieved a balance between mechanical stability and swelling behaviour, two critical parameters for active packaging applications. It was observed that increasing the concentration of CA led to a reduction in the swelling ratio, indicating the formation of a denser and more tightly crosslinked polymer network. Conversely, tensile strength improved with rising CA concentration, but only when the polymer concentration was within a moderate range, suggesting a threshold beyond which polymer saturation may hinder crosslinking efficiency.

2. The developed films, each containing different combinations of EOs, were comprehensively evaluated for their physico-chemical integrity and antimicrobial efficacy. The antioxidant activity of the films remained consistently high at both refrigerated (4 °C) and ambient (25 °C) temperatures, highlighting the stability and efficacy of the encapsulated EOs under practical storage conditions. Notably, the WVP and WVTR of the films were significantly low across all formulations, an essential characteristic for packaging materials intended to inhibit moisture ingress and preserve product quality. From a microbiological perspective, the films exhibited selective

antibacterial activity against gram-negative bacteria. These combined results affirm the films' potential for preserving moisture-sensitive and perishable food products.

3. The bioactive films were applied to ground chicken and beef samples to evaluate their real-world efficacy as packaging materials. The results revealed a differential response between the two meat types. For beef samples, the films effectively limited microbial spoilage, with all bioactive film samples maintaining microbial counts below the spoilage threshold (7 log CFU/mL) even by day 6. These findings collectively underscore the films' antioxidant capacity and their potential to extend the shelf life of high-risk meat products.

The presented work serves as a promising pilot approach toward developing eco-friendly packaging solutions that not only reduce plastic dependency but also preserve the quality and safety of food products. By offering a comprehensive evaluation of polymer–EO interactions and their impact on film performance, this study establishes a foundation for tailoring packaging materials to suit specific food systems. Although not without limitations, the films demonstrate strong potential as sustainable alternatives with active functionality. Ultimately, this research opens a practical and scientific pathway toward the future of biodegradable, bioactive packaging with customizable and scalable applications.

CONCLUSION

The present study focused on the development of crosslinked polysaccharide-based biodegradable films with encapsulated essential oils (EOs), aimed at enhancing food preservation. A structured optimization process enabled the formulation of films with controlled swelling, strong mechanical integrity, and high crosslinking efficiency. Physico-chemical and microbiological evaluations demonstrated that the films possessed low water vapour permeability, strong antioxidant properties, and selective antibacterial activity, particularly against gram-negative bacteria.

The application of these films to ground chicken and beef samples revealed their varying efficacy depending on the food matrix. Notably, microbial inhibition and oxidative stability were more pronounced in beef, likely due to lower moisture content. The films also contributed to improved colour retention and delayed spoilage indicators. Multivariate analysis supported the correlation between antioxidant potential and shelf-life extension, particularly in beef systems.

Overall, the films exhibited promising potential as eco-friendly packaging materials, offering a sustainable alternative to conventional plastics with practical functionality for perishable foods.

BIBLIOGRAPHY

1. Bishnoi, Suman et al. Quality and microbial assessment of chicken sausages treated with moringa leaf and orange peel green extracts. CyTA-Journal of Food. 2025, vol. 23, no. 1, s. 2446835.
2. Lapčík, Lubomír et al. Study of Natural Dyes' Liposomal Encapsulation in Food Dispersion Model Systems via High-Pressure Homogenization. Molecules. 2025, vol. 30, no. 8, s. 1845.
3. Soltana, Oumaima Ben et al. Improving the shelf life of minced beef by Cystoseira compressa polysaccharide during storage. International Journal of Biological Macromolecules. 2024, vol. 273, s. 132863.
4. Dos Santos, Vanessa Solfa et al. Combining Chitosan Nanoparticles and Garlic Essential Oil as Additive Fillers to Produce Pectin-Based Nanocomposite Edible Films. Polymers. 2023, vol. 15, no. 10, s. 2244.
5. Gautam, Shweta et al. Emulsion-Based Coatings for Preservation of Meat and Related Products. Foods. 2023, vol. 12, no. 4, s. 832.
6. Gautam, Shweta et al. Physicochemical characterisation of polysaccharide films with embedded bioactive substances. Foods. 2023, vol. 12, no. 24, s. 4454.
7. Mouhoub, Anouar et al. The effect of essential oils mixture on chitosan-based film surface energy and antiadhesion activity against foodborne bacteria. World Journal of Microbiology and Biotechnology. 2023, vol. 39, no. 3, s. 77.
8. Sun, Jie et al. Preparation and Application of Edible Film Based on Sodium Carboxymethylcellulose-Sodium Alginate Composite Soybean Oil Body. Coatings. 2023, vol. 13, no. 10, s. 1716.
9. Hamal, Ester Korkus et al. Structural Insights into Cellulose-Coated Oil in Water Emulsions. Langmuir. 2022, vol. 38, no. 37, s. 11171-11179.
10. Kim, SolJi et al. Effects of aging methods and periods on quality characteristics of beef. Food Science of Animal Resources. 2022, vol. 42, no. 6, s. 953.
11. Murtaja, Yousef et al. Intelligent high-tech coating of natural biopolymer layers. Advances in Colloid and Interface Science. 2022, s. 102681.
12. European Commission (EU). Regulation (EC) No 1331/2008 Establishing a common authorisation procedure for food additives, food enzymes and food flavourings 2021.
13. Mei, Luyu et al. Characterization of carboxymethyl cellulose films incorporated with Chinese fir essential oil and their application to quality improvement of Shine Muscat grape. Coatings. 2021, vol. 11, no. 1, s. 97.
14. Sharma, Shubham et al. Essential oils as additives in active food packaging. Food Chemistry. 2021, vol. 343, s. 128403.

15. Sotolářová, Jitka, Štěpán Vinter a Jaroslav Filip. Cellulose derivatives crosslinked by citric acid on electrode surface as a heavy metal absorption/sensing matrix. Colloids and Surfaces A: Physicochemical and Engineering Aspects . 2021, vol. 628, s. 127242.

16. Sun, Rui et al. Effect of basil essential oil and beeswax incorporation on the physical, structural, and antibacterial properties of chitosan emulsion based coating for eggs preservation. Lwt. 2021, vol. 150, s. 112020.

17. Cai, Luyun, Yaru Wang a Ailing Cao. The physiochemical and preservation properties of fish sarcoplasmic protein/chitosan composite films containing ginger essential oil emulsions. Journal of Food Process Engineering. 2020, vol. 43, no. 10. ISSN 0145-8876.

18. Dalvandi, Fereshteh et al. Effect of vacuum packaging and edible coating containing black pepper seeds and turmeric extracts on shelf life extension of chicken breast fillets. Journal of Food and Bioprocess Engineering. 2020, vol. 3, no. 1, s. 69-78.

19. Huang, Mingyuan et al. Effects of nanoemulsion-based edible coatings with composite mixture of rosemary extract and ε-poly-L-lysine on the shelf life of ready-to-eat carbonado chicken. Food Hydrocolloids. 2020, vol. 102, s. 105576.

20. Simsek, Meric, Belma Eke a Hande Demir. Characterization of carboxymethyl cellulose-based antimicrobial films incorporated with plant essential oils. International Journal of Biological Macromolecules. 2020, vol. 163, s. 2172-2179.

21. Ghorpade, Vishwajeet Sampatrao et al. Citric acid crosslinked carboxymethylcellulose-polyvinyl alcohol hydrogel films for extended release of water soluble basic drugs. Journal of Drug Delivery Science and Technology. 2019, vol. 52, s. 421-430.

22. Nordin, Nurul A. et al. Citric acid cross-linking of carboxymethyl sago starch based hydrogel for controlled release application. Wiley Online Library, 2018. 1800086 s.

23. Catauro, Michelina et al. Chemical analysis and anti-proliferative activity of Campania Thymus Vulgaris essential oil. Journal of Essential Oil Research. 2017, vol. 29, no. 6, s. 461-470.

24. Danish, Muhammad et al. Response surface methodology based optimized purification of the residual glycerol from biodiesel production process. Chiang Mai J.Sci . 2017, vol. 44, no. 4, s. 1570-1582.

25. Gao, Hongfang, Hui Yang a Chuang WANG. Controllable preparation and mechanism of nano-silver mediated by the microemulsion system of the clove oil. Results in Physics. 2017, vol. 7, s. 3130-3136.

26. Hassoun, Abdo a Özlem Emir Çoban. Essential oils for antimicrobial and antioxidant applications in fish and other seafood products. Trends in Food Science & Technology. 2017, vol. 68, s. 26-36.

27. Juncu, Gheorghe et al. Drug release kinetics from carboxymethylcellulose-bacterial cellulose composite films. International Journal of Pharmaceutics. 2016, vol. 510, no. 2, s. 485-492.

28. Topala, Carmen Mihaela a Lavinia Diana Tataru. ATR-FTIR Study of thyme and rosemary oils extracted by supercritical carbon dioxide. Rev.Chim. (Bucharest). 2016, vol. 67, s. 842-846.

29. Rachmawati, Novalia, Radestya Triwibowo a Roni Widianto. Mechanical properties and biodegradability of acid-soluble chitosan-starch based film. Squalen Bulletin of Marine and Fisheries Postharvest and Biotechnology. 2015, vol. 10, no. 1, s. 1-7.

30. Shen, Zhu a Donatien Pascal Kamdem. Development and characterization of biodegradable chitosan films containing two essential oils. International Journal of Biological Macromolecules. 2015, vol. 74, s. 289-296.

31. Hu, Bin. Biopolymer-based lightweight materials for packaging applications. Lightweight Materials from Biopolymers and Biofibers. 2014, s. 239-255.

32. ASTM International. ASTM standard E96, standard test methods for water vapor transmission of materials. West Conshohocken, PA: , 2013.

33. Valderrama Solano, Andrea Carolina a Cecilia De Rojas Gante. Two different processes to obtain antimicrobial packaging containing natural oils. Food and Bioprocess Technology. 2012, vol. 5, s. 2522-2528.

34. Speranza, Barbara a Maria Rosaria Corbo. Essential oils for preserving perishable foods: possibilities and limitations. Application of Alternative Food-Preservation Technologies to Enhance Food Safety and Stability. 2010, vol. 23, s. 35-37.

35. ASTM International. ASTM standard D882, standard test method for tensile properties of thin plastic sheeting. West Conshohocken, PA, 2009.

36. Demitri, Christian et al. Novel superabsorbent cellulose-based hydrogels crosslinked with citric acid. Journal of Applied Polymer Science. 2008, vol. 110, no. 4, s. 2453-2460.

37. ASTM International. ASTM standard D3418, melting point by DSC testing services. West Conshohocken, PA, 2003.

38. ASTM: D-882-91 method. In annual book of ASTM standards. Philadelphia: American Society for Testing and Materials, 1996Standard test methods for tensile properties of thin plastic sheeting, D882-91.

LIST OF SYMBOLS AND ABBREVIATIONS USED

1.	EO	Essential Oil
2.	NA	Natural Antioxidants
3.	EU	European Union
4.	EF	Edible Films
5.	EC	Edible Coating
6.	DOE	Design of Experiment
7.	CCD	Central Composite Design
8.	RSM	Response Surface Methodology
9.	CMCNa	Sodium-carboxymethyl cellulose
10.	HEC	Hydroxyethyl cellulose
11.	CA	Citric Acid
12.	T80	Tween 80
13.	DW	Distilled Water
14.	TS	Tensile Strength
15.	EM	Young's Modulus of Elasticity
16.	EB	Elongation at Break
17.	ASTM	American Society for Testing and Materials
18.	TGA	Thermogravimetric Analysis
19.	WVP	Water Vapour Permeability
20.	WVTR	Water Vapour Transmission Rate
21.	TBARS	Thio barbituric acid

LIST OF IMAGES

LIST OF TABLES

BIOGRAPHY OF THE AUTHOR

Name and Last name:	Shweta Gautam
Date of birth:	30.09.1995
Address:	HNo. 200 Sector 5 Part-6, Gurgaon, Haryana, India
E-mail:	gautam@utb.cz
Tel.:	+420 777097387

Education:

2021–2025: Tomas Bata University, Faculty of Technology- doctoral studies in Food Technology

2018–2020: Pondicherry University, Faculty of Technology- Masters in Food Science and Technology

2015–2018: Delhi University, Faculty of Technology, Bachelors in Food Technology

Work Placements:

2023: Erasmus+, Polish Academy of Sciences, Jerzy Haber Institute of Catalysis and Surface Chemistry, Krakow, Polsko, 2 months

2019: FICCI Food Research Analysis Centre, Dwarka, India, 1 month

2018: Packing and quality assurance at Coca-Cola (Moon Beverages), UP, India, 1 month

PROJECT ACTIVITIES:

2021-Influence of Technological Trends on Quality and Properties of Selected Foods, IGA/FT/2021/004, co-investigator

2022-Technological Trends Affecting the Quality and Properties of Selected Foods, IGA/FT/2022/005, co-investigator

2023-Comprehensive evaluation of dispersion systems with focus on physicochemical and mechanical properties of food products, IGA/FT/2023/007, co-investigator

2024-The influence of various food additives and technological parameters on selected properties of food systems, IGA/FT/2024/005, co-investigator

2025- Evaluation of the influence of food additives and technological parameters on the physicochemical and mechanical properties of foods, IGA/FT/2025/007, co-investigator

---

List of the Author's Publications:

1. Chemical and Coloristic Profiles of Red and Rosé Wines from Domestic Production and Wineries of Moravia Wine Region: Tereza Huskova, Lubomir Lapcik; Tomas Valenta; Shweta Gautam; Barbora Lapcikova; Miroslav Fisera| 2025-05-05| DOI: 10.19080/JOJHA.2025.05.555664
2. Pharmacological Significance of Boraginaceae with special insights into Shikonin and its potential in the food industry: Shweta Gautam; Lubomir Lapcik; Barbora Lapcikova|2024-04-27| DOI: https://doi.org/10.3390/foods13091350
3. Physicochemical characterisation of Polyshaccharide films with embedded bioactive substances: Shweta Gautam; Lubomir Lapcik; Barbora Lapcikova; David Řepka; Lilianna Szyk-Warszynsk |Foods| 2023-12-12 | DOI: 10.3390/foods12244454

4. Emulsion based coatings for meat and related products: Shweta Gautam; Lubomír Lapčík; Barbora Lapčíková; Robert Gál| Foods| 2023 | DOI: 10.3390/foods12040832
5. Physico-chemical study of curcumin and and its application in O/W/O Multiple emulsions: Kristýna Opustilová; Barbora Lapčíková; Lubomír Lapčík; Shweta Gautam; Tomáš Valenta; Peng Li| 2023|Foods| DOI: 10.3390/foods12071394
6. Amaranthus paniculatus (Rajgeera) a nonconventional source of starch: effect of oxidation and heat moisture treatment and its application in edible film: Pooja Yadav; Shweta Gautam; S. John Don Bosco| Biomass Conversion and Biorefinery| 2023-06-15 | DOI: 10.1007/s13399-023-04493-2
7. Study of mechanical properties of epoxy/graphene and epoxy/ halloysite nanocomposites: Lubomír Lapčík; Harun Sepetcioğlu; Yousef Murtaja; Barbora Lapčíková; Martin Vašina; Martin Ovsík; Michal Staněk; Shweta Gautam| Nanotechnology Reviews 2023-03-16 | Journal article DOI: 10.1515/ntrev-2022-0520
8. Acoustic and mechanical testing of commercial cocoa powders: Lubomir Lapcik; Barbora Lapcikova; Shweta Gautam; Martin Vašina; Tomáš Valenta; David Řepka; Klára Čépe; Ondřej Rudolf|International Journal of Food Properties 2022-12-31 | DOI: 10.1080/10942912.2022.2127760
9. Intelligent high-tech coating of natural biopolymer layers: Yousef Murtaja , Lubomir Lapcík, Barbora Lapcíkova´, Shweta Gautam, Martin Vasina, Lubomir Spanhel, Jakub Vlcek| Advances in Colloid and Interface Science|2022-06 |DOI: 10.1016/j.cis.2022.102681
10. A Physicochemical study of the Antioxidant activity of corn silk extracts: Lubomir Lapcik, David Řepka, Barbora Lapcikova, Daniela Sumczunski,

Shweta Gautam; Peng Li; Tomáš Valenta| Foods| 2023| DOI: https://doi.org/10.3390/foods 12112159

Papers in conference proceedings:

1. Physico-chemical and Microbiological analysis of thyme-CMC emulsions for shelf-life extension of Shrimps: Shweta Gautam, Tereza Hůsková, Lubomir Lapčík, Barbora Lapčíkova|2024|DOI: 10.15414/2024.sqf24-psp
2. Study of physical properties of commercial cocoa powders by acoustic and mechanical evaluation: Lubomir Lapčík, Barbora Lapčíkova, Shweta Gautam| 2023| page: 254-258
3. Study of physico-chemical characteristics of selected wines from the Bzenec Moravia region: Shweta Gautam, Tereza Hůsková, Tomáš Valenta, Barbora Lapcikova, Lubomir Lapcik| 2022| DOI:10.15414/2022.sqf22-psp

Shweta Gautam

Natural antioxidants and their use in Food Technology

Přírodní antioxidanty a jejich využití v Potravinářství

Doctoral Thesis Summary

Published by: Tomas Bata University in Zlín,
nám. T. G. Masaryka 5555, 760 01 Zlín

Edition: published electronically
Typesetting by: Shweta Gautam, Ph.D.
This publication has not undergone any proofreading or editorial review

Publication year: 2025
First Edition

ISBN: 978-80-7678-350-8